Hydrodynamic forces on monopiles with secondary structures.

Numerical approach

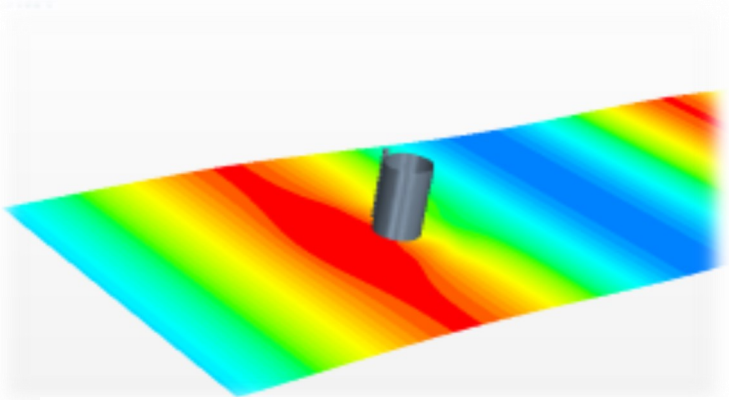

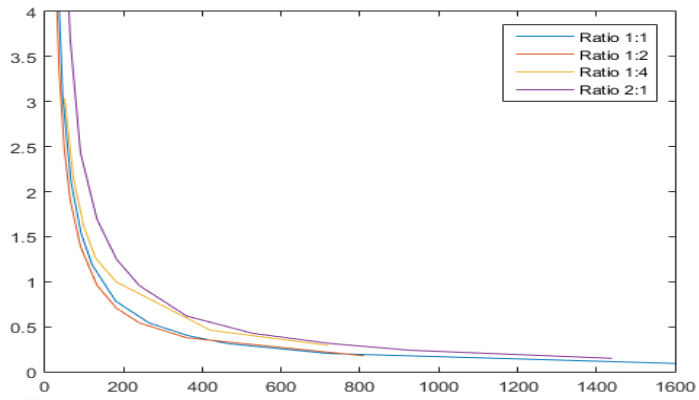

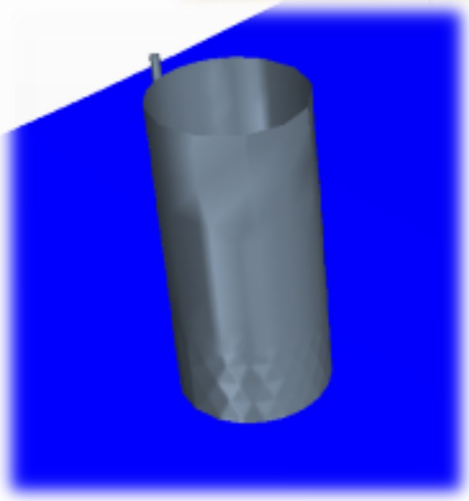

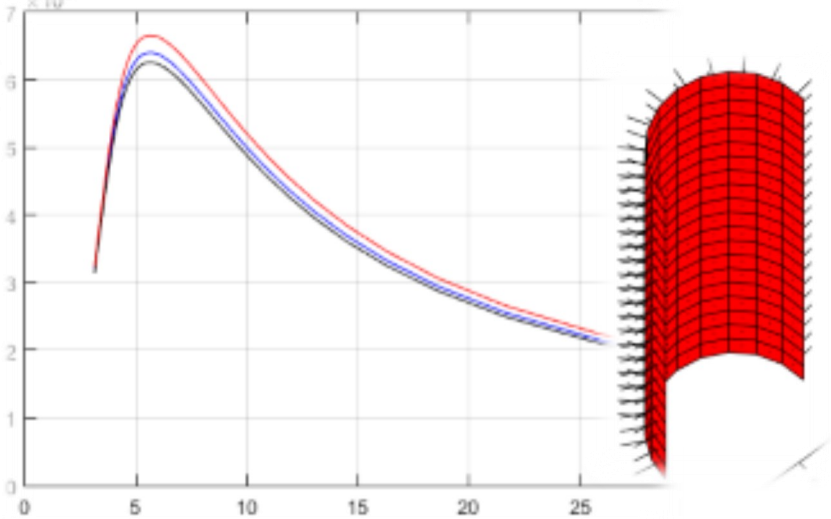

Master Thesis

Civil and Structural Engineering

Aalborg University

Michael Nygaard

June 2016

AALBORG UNIVERSITET
STUDENT REPORT

School of Engineering and Science

Department of Civil Engineering
Sofiendalsvej 9-11
9200 Aalborg SV
http://www.civil.aau.dk

Title:

Hydrodynamic forces on monopiles with secondary structures.
Numerical approach

Theme:

Master Thesis
Civil and Structural Engineering

Project period:

M.Sc. 4th semester. Spring 2016

Author:

Michael Nygaard

Supervisor

Morten Mejlhede Kramer

Editions: 6
Number of pages: 35
Amount of appendix: 3
Annex-Disc: 5
Hand-in 08-06-2016

Synopsis:

The main purpose of this project was to investigate the usability of numerical models in order to determine the hydrodynamic forces on a monopile with a secondary structure. The numerical models used was BEM models and CFD models.
In the analysis, a analytical solution by MacCamy and Fuchs was used to calibrate the BEM models because they are based on the same theory and should trend towards the same results. This was done with a convergence analysis. Skewness of the elements was also considered.
For the CFD models the Volume of Fluid (VOF) method was used and using the program Star-CCM+ it is possible to generate waves in the domain. Models with and without the secondary structure was analysed using nine different wave conditions with varying wave height and wave period. The wave conditions are based on waves used in physical model tests.
Finally the different methods are compared to each other and physical model tests. The comparison shows that BEM might not be a suitable method to determine forces because drag is a factor when considering monopiles. CFD consider drag and gives results closer to the model tests. But there are still further studies to be made in order to determine the viability of numerical models, but there is potential.

Preface

This report represents the Master Thesis created by Michael Nygaard as part the M.Sc. on Civil and Structural Engineering at Aalborg University. The project is made in the period from 01-02-2016 to 08-06-2016.

Acknowledgement

I would like to send a thanks to Ammar Galib Al-Faili for performing the physical model tests used in this project. I would also like thanks to Mads Sønderstrup Røge for counseling in the initial phases of the making the CFD-models.

Reading guide

The report is built up in such a way that it only comprises the basis of the theories and the possible limitations of these and how these limitations are treated in order to get valid results for a given scenario.

Source Citation

Source references are developed by the Harvard method and refer to the full source list at the back of the report. A passive source will be indicated by the text's end as follows: [Surname, Year]. By an active source, for example an website, it will be referred in the text of the specific date of the entry.
In cases when referring to a certain code or standard with no specific author, then the publisher will be listed as author, e.g. [IEC 61400-3, 2009].

Figures, tables and equations

Figures, tables and equations in the report will be numbered under which chapter they belong and which number in the sequence of tables, figures and equations they are in chapter. As an example, "Fig 5.2" can be found in Chapter 5 and is the second figure. Equations numbers appear in parentheses and shifted to the right side of the document.

Appendix

Appendix is divided in accordance to letters of the alphabet and can be found in the back of the report.

Annex

The annexes will be available on a DVD that will be available on the reports rear side. This DVD will be referred as "Annex-Disc" and will contain all the calculations underlying the reports contents. The content of this DVD can be found in Appendix C.

Contents

1 Introduction **1**

1.1 Problem formulation 1

1.2 Construction 2

1.3 Approach 4

2 MacCamy and Fuchs **5**

2.1 Theory 5

2.2 Results 8

3 Boundary Element Method **9**

3.1 Theory 9

3.2 Programs 9

3.3 Monopile model 10

3.4 Boat Landing model 14

4 CFD-method **19**

4.1 Theory 19

4.2 Model considerations 20

4.3 Data treatment 24

4.4 Results 25

5 Comparison **29**

5.1 Physical model tests 29

5.2 Monopile model 31

5.3 Boat Landing model 31

6 Conclusion **33**

Bibliography **35**

A Results Convergence Monopile Ratio 1:1

B Data treatment of Experiments, Monopile Model

C Annex Disc

Introduction 1

When establishing offshore wind farms, foundations of the wind turbines are a huge expense on the total budget. Therefore it is worthwhile to make custom foundations for each turbine depended on the site conditions. There are different types of foundations being used today, such as:

- Steel monopile foundations
- Concrete gravity based foundations
- Jacket structures
- Tripod foundations
- Bucket foundations

The three latter types are either used for tender situations or concept and preliminary design which are rarely used. The first two are the most common. [COWI, 2015]

In this project the focus will be on monopile foundations. A monopile foundation consists of two main components, a monopile and a transition piece. The monopile is a steel cylinder with a diameter that usually range from 4-6 m depending on the specific project. The length is specifically designed for each location depending on the geotechnical conditions at the location and water depth. The transition piece is a structure being put on the monopile and has all the necessary things for the wind turbine. Among these things is a boat landing, so the wind turbine is accessible for inspection and maintenance. Other things are J-tubes for cables to be protected and have easy access to the turbine.

The design procedures of these foundations are based on comprehensive studies and experience from the oil and gas industry. The main difference in relation to wind turbines is that oil and gas platforms are much larger than the wind turbine foundations and some of the premises for the calculations might no longer be valid and in order to counteract this, some conservative estimation are used. Some of these are still present in the current design codes.

1.1 Problem formulation

Design standards are considered to potentially be too conservative when dealing with hydrodynamic load coefficients related to secondary structures. This conservatism leads to more expenses on constructions and by reviewing the design standards, the construction costs of offshore wind turbines could potentially decrease, if this conservatism can be verified.

The main purpose of this project is to investigate the hydrodynamic forces acting on a monopile with secondary structures, in order to verify or disprove the current design standards on the subject. The approach taken to determine these forces is a numerical modelling approach, where loads are modelled with and without the presence of secondary structures.

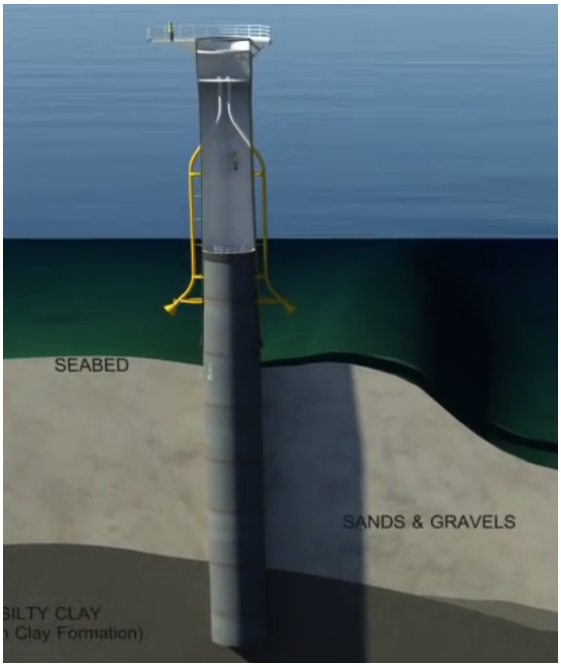

Fig 1.1. Cross-section of a monopile foundation. [COWI, 2010]

Fig 1.2. Transition piece with visible secondary structures, e.g. boat landing. [COWI, 2010]

The forces calculated using these numerical models will be compared to a analytical solution, MacCamy and Fuchs, and experimental results, which are more extensively treated in another project.

Two different numerical models will be considered: One model based on the Boundary Element Method (BEM) and a Computational Fluid Dynamic-model (CFD), which is based on the Finite Volume Method (FVM).

1.2 Construction

This project will evaluate a monopile construction with secondary structure which in real life could be a boat landing, j-tubes, etc. Fig 1.3 shows a sketch of the construction and the magnitude of the measures are listed in Table 1.1. Measures for a model with a 1:40 scale are also listed in the table.

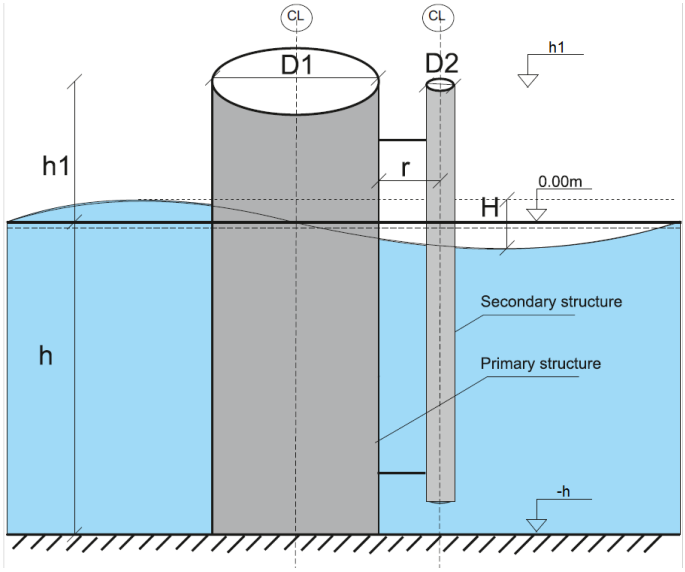

Fig 1.3. The simplified structure with all the parts.

		Full Scale	Model Scale	
$D1$	=	6.4 m	0.16 m	Diameter of primary structure
$D2$	=	0.4 m	0.01 m	Diameter of secondary structure
h	=	18.0 m	0.45 m	Water depth, to MWL
$h1$	=	12.0 m	0.30 m	Height of structure above MWL
r	=	1.5 m	0.1175 m	Distance from primary structure to center of secondary
H				Wave height

Table 1.1. Dimensions of the construction in full and model scale.

Two different models will be considered in this project. One model with no secondary structure which will be referred to as Monopile model. And one model with secondary structure on the side relative to wave front, see Fig 1.4 which will be referred to as Boat Landing model.

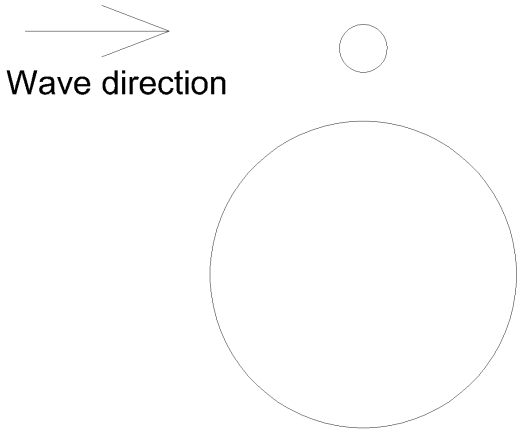

Fig 1.4. Orientation of Boat Landing model.

1.3 Approach

Analysis of the construction with and without the secondary structure will be performed. In order to solve the points mentioned in previous section, different methods are used to analyse forces on the structures and four different methods are used.

MacCamy and Fuchs	This is an analytical method to calculate the wave forces on a large cylindrical structure. This can only be used when considering the Monopile model.
BEM	This is a computational solution, which is based on the same conditions as MacCamy and Fuchs, but more advanced construction can be modelled and solved numerically.
CFD/FVM	This is a method in which the governing equations are solved in an element wise manor, the volume of water and the construction in 3D is modelled. Waves are then generated and the forces on the construction can be analysed.
Physical model testing	This is laboratory experiments on a scaled model of the construction performed in a wave basin.

Normally would Morisons equations would be used to determine the wave forces, but in this project only MacCamy and Fuchs would be used as analytical approach.

MacCamy and Fuchs 2

In this chapter the analytical method to calculate wave forces on a cylindrical structure based on MacCamy and Fuchs [1954] is evaluated.

When considering wave forces on off-shore structures, three phenomena have influence on the total forces, drag, inertia and diffraction. Each of these are dominant in individual cases. Drag is dominant when considering small and slender structures, inertia is dominant when considering large structures and diffraction become dominant when considering very large structures. MacCamy and Fuchs is based on diffraction theory and can be used when considering very large structures, which are defined as structures with a ratio of body size (D) to wave length (L) being larger than 0.2 (D/L $>$ 0.2). [DNV-RP-C205, 2010]

The construction don't fully live up to this requirement and Morisons equation would be more accurate. This theory is also basis for BEM and this makes comparison between the method straight forward. Through the report, MacCamy and Fuchs will also be referred to as MCF.

2.1 Theory

MacCamy and Fuchs utilizes an assumption of linear wave theory which is valid when the wave height is sufficiently small. This is done in order to eliminate some aspects which adds complexity, but not significantly influences the results.

Linear theory assumes waves to follow a cosine curve and because of a direct correlation between surface elevation and force leads to the force also following a cosine curve. This means the surface elevation and force can be expressed as Eq. (2.1) and (2.2). An illustration of the force can be seen on Fig 2.1. In linear theory the following is also true, $a_{\eta,max}$ = H/2 and $a_f = F_{max}$. Linear theory uses the assumption of small wave height (H/L $\ll$ 1), but already at H/L $>$ 0.01 the assumption begins to be invalid. [Andersen et al., 2014]

$$\eta(t) = a_\eta \cos(\omega t) \tag{2.1}$$

$$f(t) = a_f \cos(\omega t + \delta) \tag{2.2}$$

$\eta(t)$	Surface elevation	[m]
a_η	Surface amplitude	[m]
$f(t)$	Force	[N]
a_f	Force amplitude	[N]
ω	Wave frequency	[Hz]
t	Time	[s]
δ	Phase	[-]

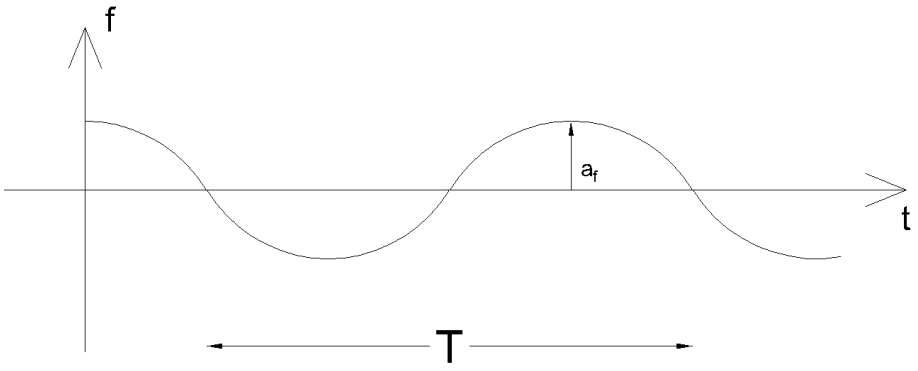

Fig 2.1. Time series of force in simple linear case.

Linear theory can be summarized in Fig 2.2. This shows that in the fluid domain the Laplace equation is fulfilled, and there are boundary condition such as no flow through the bottom, flow through the sides and free surface on the top. Having a structure in the fluid domain introduces the boundary condition of no flow through the walls of the structure, illustrated on Fig 2.3

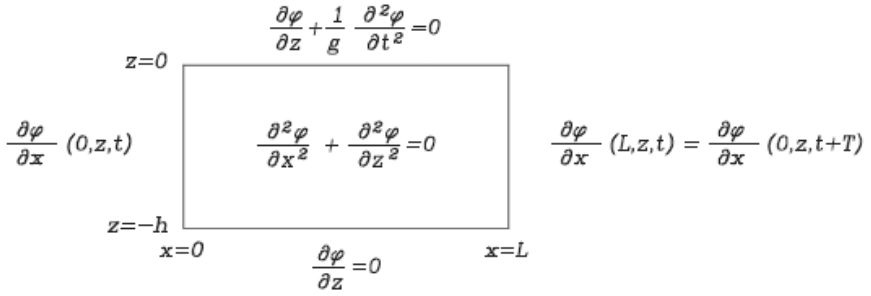

Fig 2.2. Summary of Linearised Problem.[Andersen et al., 2014]

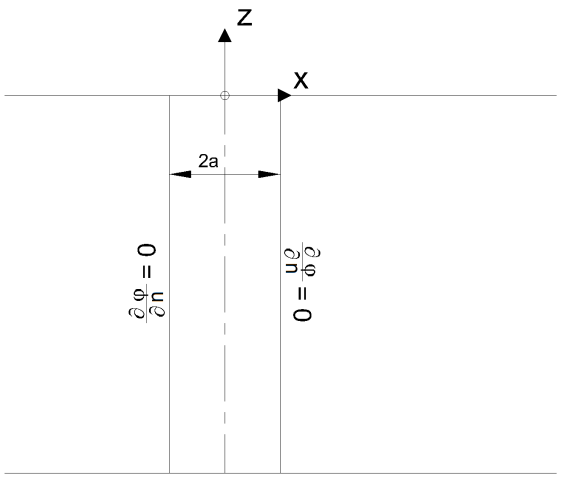

Fig 2.3. Boundary conditions on a structure in the fluid domain.

When placing a structure in the domain, the waves hitting the structure will scatter and reflect into the domain. Because of linear theory and using the superposition priciple, velocity potential can then be represented as:

$$\phi = \phi_w + \phi_s \tag{2.3}$$

ϕ	Total velocity potential
ϕ_w	"Incident wave" potential
ϕ_s	"Scattered wave" potential

The incident wave potential fulfill all the boundary conditions can be expressed in the complex form as:

$$\phi_w = A\frac{\cosh(k(z+d))}{\cosh(kd)}e^{i(kx-\omega t)} \tag{2.4}$$

$A = \quad igH/2\omega$

The body surface boundary condition be expressed as:

$$\frac{\partial \phi_s}{\partial n} = -\frac{\partial \phi_w}{\partial n} \tag{2.5}$$

The pressure and thereby the forces can then be calculated based on the linearised Bernoulli equation when both incident wave potential and scatted wave potential are know:

$$p = -\rho g z - \rho\frac{\partial \phi}{\partial t} \tag{2.6}$$

In order to determine the incident and scattered wave potential, MacCamy and Fuchs then utilizes a series Bessel functions. [Sarpkaya and Isaacson, 1981]

All this ends up with a function for the total force on the structure:

$$\begin{aligned} F =& \frac{\pi}{8}\rho g H D^2 \tanh(kd) C_m \cos(\omega t - \delta) \\ C_m =& \frac{4A(ka)}{\pi(ka)^2} \\ A(ka) =& \left[J_1'^2(ka) + Y_1'^2(ka)\right]^{-1/2} \\ \delta =& -\tan^{-1}\left[Y_1'(ka)/J_1'(ka)\right] \end{aligned} \tag{2.7}$$

F	Total force on structure	[N]
ρ	Density of fluid (Water)	[kg/m^3]
H	Wave height	[m]
D	Diameter of cylinder	[m]
ω	Wave frequency	[Hz]
$J_m'(ka)$	Bessel function of order m	[–]
$Y_m'(ka)$	Bessel function of order m	[–]

2.2 Results

The horizontal force per wave amplitude on the cylinder, expressed as Eq. (2.8), can then be plotted as a function of the wave period, which is shown in Fig 2.4. For this case the full scale monopile is used. This method of measuring force will be used throughout the report.

$$F_{unit} = \frac{a_f}{a_\eta} \tag{2.8}$$

F_{unit}	Force per wave amplitude	[N/m]
a_f	Force amplitude	[N]
a_η	Surface amplitude	[m]

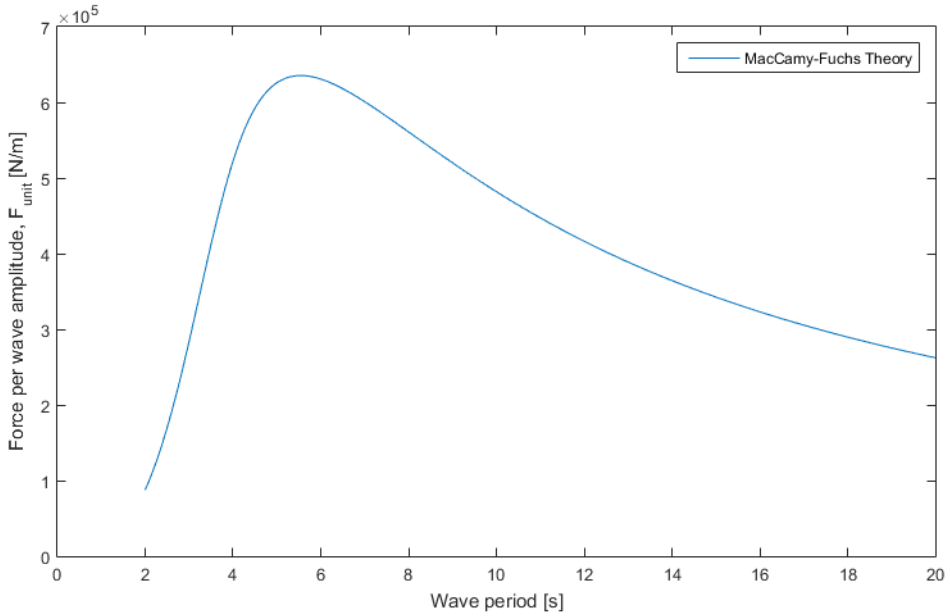

Fig 2.4. Horizontal force per wave amplitude on given structure in relation to wave period.

Boundary Element Method 3

In this chapter the forces on the construction are analysed using the Boundary Element Method (BEM). This is used when constructions become too complex for analytical methods.

3.1 Theory

BEM is generally based on the same theory as MacCamy and Fuchs, which was described in Section 2.1, but this method uses sources to fulfil the boundary condition of no flow through the wall of on structure.

By adjusting the strength of the source in each element it is possible to fulfil the boundary condition on the structure of no flow through the walls. From the strength of the source, forces on the element can be calculated using Bernoulli.

3.2 Programs

For this analysis, two different programs are used and the solutions from both are evaluated.

3.2.1 Nemoh

Nemoh is an open-source program which is developed by LHEEA (Laboratoire de recherche en Hydrodynamique, Énergétique et Environnement Atmosphérique) at the engineering school Ecole Centrale Nantes in France. Being open-source it is free to use and it is possible to modify the code in order to get the most out the program.

Nemoh consists of three programs which each have a certain purpose in the calculation. What each program does can be seen in Fig 3.1.

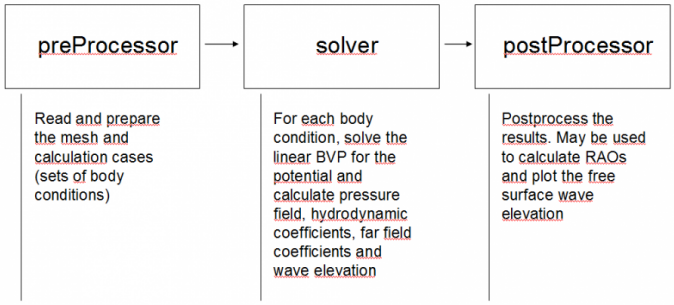

Fig 3.1. The three program of which Nemoh consist.[LHEEA, 2016]

LHEEA has also made some MATLAB code which make it possible to run Nemoh in a MATLAB environment.

They have also develop meshing tools, also in MATLAB, which can make it simple axis-symmetric models. Because the models in this projects consist primarily of cylinders, this is an ideal tools to generate the meshes. As part of this meshing tools is also a program which converts the mesh into the format that Nemoh can read.

For this project, Nemoh is primarily used in the MATLAB environment and the meshes are made using a script made from the meshing tools.

3.2.2 Wamit

Wamit is a commercial program and therefore require a license in order to use the program. For this project, the license is provided by Aalborg University.

The program consist of a series of programs which are combined into a single "run" file. This file reads a series of input files which states the mesh and the overall geometry.

The meshes used for Wamit are the same as for Nemoh in order to make the results comparable. In order to make sure that similar meshes are used in both programs, a MATLAB code, which is part of a toolbox for Nemoh, converts a mesh from the format used by Nemoh to the format used by Wamit.

3.3 Monopile model

The meshes being generated are only of half the structure because both programs can operate with symmetry and this is used in order to keep the number of elements down. In the models in the BEM-method the structure is only modelled up to MWL.

The code used to generate the meshes uses a specified division of the perimeter and height. A rule of thumb is to have the ratio height and width of each element to be 1:1 in order to get the best results. But the influence of this ratio is also considered when choosing the appropriate mesh for this analysis.

For this model many different mesh will be analysed in order to determine how fine a mesh is needed for the results to converge. The convergence is made by considering the error between the forces calculated using MCF and the BEM-model. This is because they are based on the same theory and should yield the same results.

The different meshes are named according to the number of elements there are around the perimeter in the model, e.g. Mesh-10 has 10 elements around the perimeter. The meshes considered ranges from very rough meshes with 3 elements around the perimeter to very fine with 30 elements around the perimeter. Illustrations of two different mesh can by seen in Fig 3.2 and 3.3.

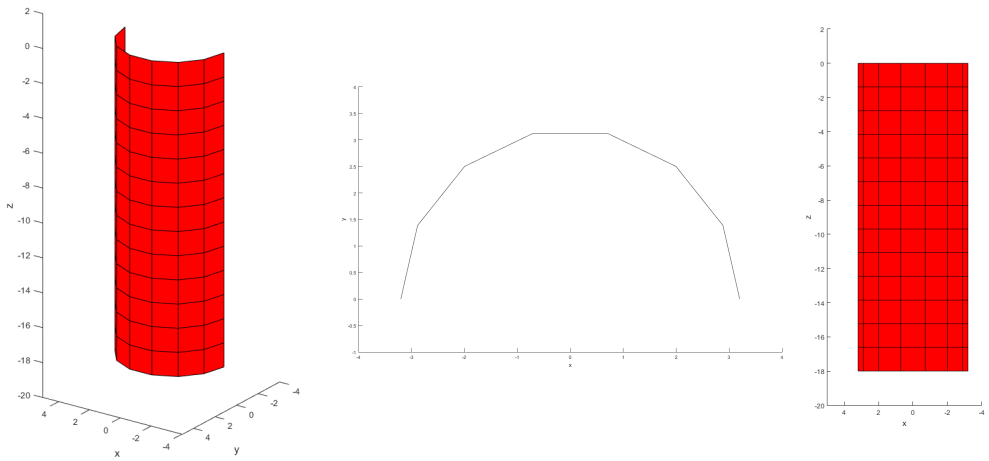

Fig 3.2. Views of Mesh-7. Perspective - Top view - Front view.

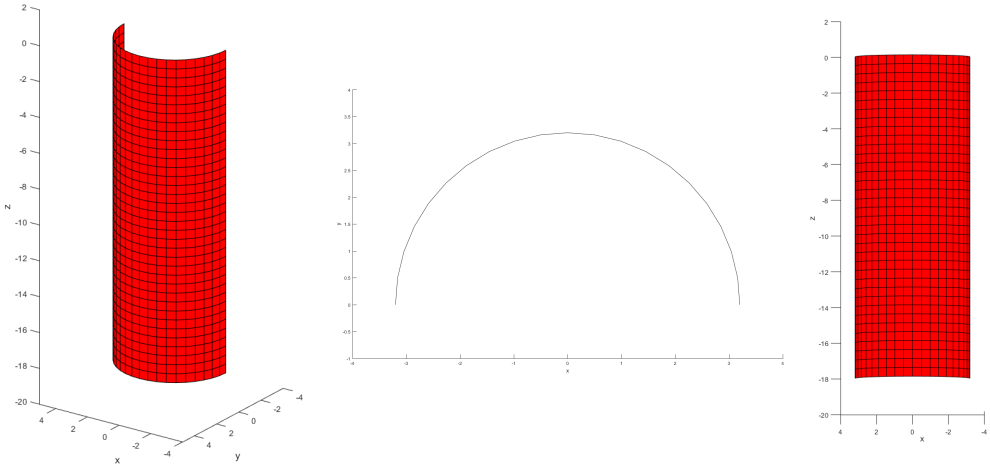

Fig 3.3. Views of Mesh-20. Perspective - Top view - Front view.

3.3.1 Convergence analysis

Each mesh is analysed considering wave frequencies ranging from 0.1 to 2 Hz and the forces using MCF are calculated considering the same wave frequencies. The percentage error in relation to MCF is calculated for each point. The mean of these errors is the one being considered in the convergence analysis.

In Table 3.1 are listed the meshes analysed with the number of elements in each model and the error for both Nemoh and Wamit. Fig 3.4 and 3.5 displays the error in relation to number of elements for Nemoh and Wamit respectively. In Appendix A the force curves for MCF, Nemoh and Wamit are plotted to display the difference. This is for all meshes.

Mesh Name	No. of elements	Error Nemoh [%]	Error Wamit [%]
Mesh−3	18	4.83	7.85
Mesh−4	32	0.96	4.49
Mesh−5	45	0.86	3.06
Mesh−6	66	1.19	2.11
Mesh−7	91	1.35	1.55
Mesh−8	120	1.41	1.19
Mesh−10	180	1.38	0.78
Mesh−12	264	1.28	0.54
Mesh−14	364	1.17	0.40
Mesh−16	464	1.05	0.31
Mesh−20	720	0.86	0.20
Mesh−30	1620	0.55	0.09

Table 3.1. Meshes with the error from both Nemoh and Wamit compared to MCF.

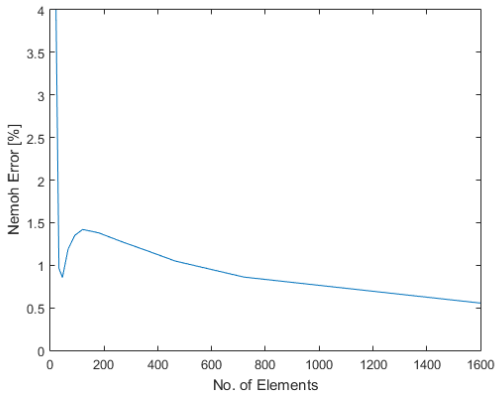

Fig 3.4. Error between Nemoh and MCF in relation to No. of elements.

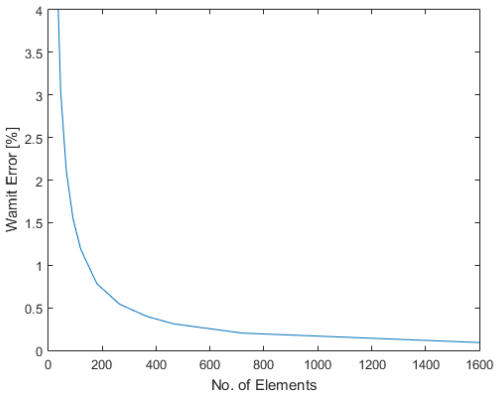

Fig 3.5. Error between Wamit and MCF in relation to No. of elements.

3.3.2 Skewness analysis

A method to reduce the number of elements in the model is by increasing the ratio between height and width of the elements. Previous this ratio was set to approx. 1:1, but in this section this ratio is changed. The ratio is both increased, making the height larger than the width, and decreased, making the height smaller than the width. The ratios considered are 2:1, 1:2 and 1:4 apart from the original ratio of 1:1. The differences in the meshes are illustrated in Fig 3.6.

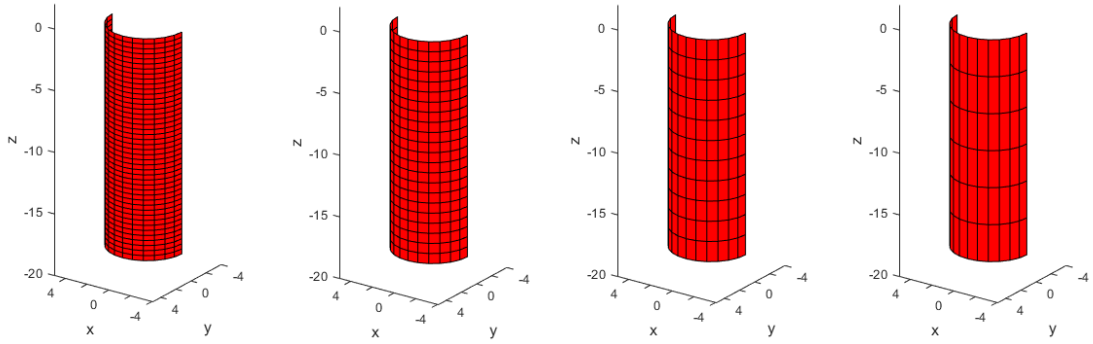

Fig 3.6. Mesh-12 with ratio of: 2:1 , 1:1 , 1:2 , 1:4.

In Table 3.2 are shown selected meshes with the influence of the skewness on both number of elements and error in Wamit and Nemoh. Also in Fig 3.7 - 3.10 the errors are plotted for all tested meshes in relation to both number of elements and discretion of the semi-circle.

Mesh Name	Ratio	No. of elements	Error Nemoh [%]	Error Wamit [%]
Mesh-10	2 : 1	360	1.58	0.62
	1 : 1	180	1.38	0.78
	1 : 2	90	1.37	1.39
	1 : 4	50	2.70	3.04
Mesh-12	2 : 1	528	1.42	0.43
	1 : 1	264	1.28	0.54
	1 : 2	132	1.19	0.96
	1 : 4	72	2.05	2.16
Mesh-14	2 : 1	728	1.27	0.31
	1 : 1	364	1.17	0.40
	1 : 2	182	1.06	0.70
	1 : 4	98	1.63	1.62

Table 3.2. Meshes with the error from both Nemoh and Wamit compared to MCF.

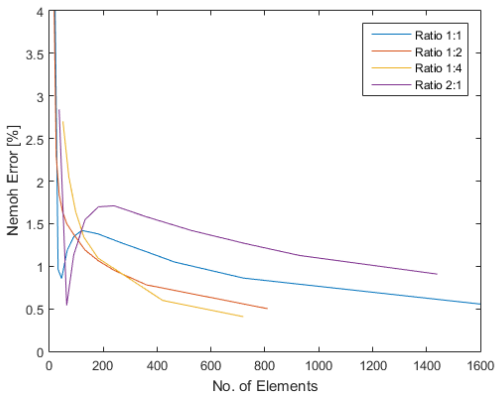

Fig 3.7. Effect of skewness on error for Nemoh in relation to No. of Elements.

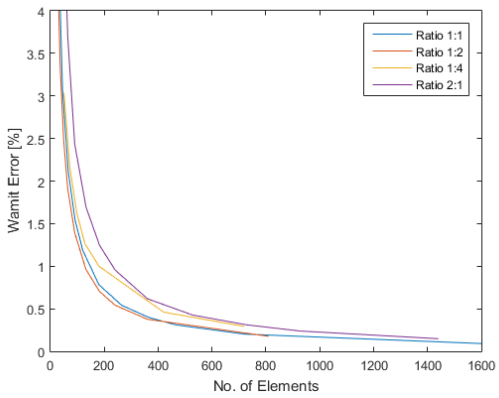

Fig 3.8. Effect of skewness on error for Wamit in relation to No. of Elements.

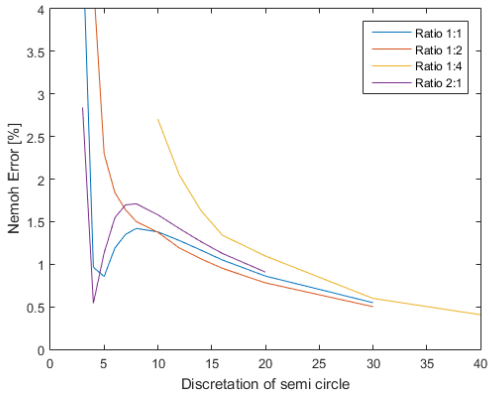

Fig 3.9. Effect of skewness on error for Nemoh in relation to discretion of the semi-circle.

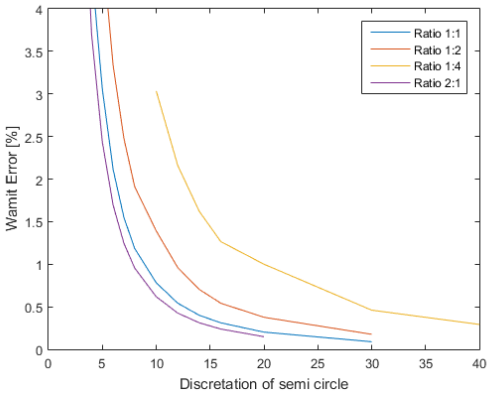

Fig 3.10. Effect of skewness on error for Wamit in relation to discretion of the semi-circle.

From the figures it can be seen that Wamit gives approximately the same error for ratio of 1:1 and 1:2 in relation to the number of elements and 2:1 and 1:4 gives higher error. In relation to the discretion of the semi-circle, the mesh with ratio of 2:1 gives lowest error. From this it can be deduced that Wamit gives the best results when having a mesh with many elements and a ratio close to 1:1.

When looking at Nemoh the error in relation to discretion of the semi-circle it indicates that Nemoh benefits from a good discretion of the semi-circle and isn't as susceptible to the influence from the skewness as Wamit appears to be. This can also be seen when looking at the error from Nemoh in relation to number of elements. Here it shows that higher skewness gives better results, which seems counter-intuitive. Another thing worth noticing is that Nemoh also shows an odd convergence when modelling with a skewness of 2:1 and 1:1. For ratios 1:2 and 1:4 gives a more expectable convergence curve. This could indicate that a error in either the program or the meshing e.g Nemoh can't handle meshes where the width of the elements are larger than the height.

3.3.3 Choosing a mesh

In order to be able to choose an acceptable mesh, it must be determined how large an error can be accepted from the results. In this case an error of 0.5% would be considered an acceptable result and for some parts an error of 1% can be accepted.

Based on this and with the consideration of both the fineness of the mesh and the skewness of the elements, Mesh-20 with a skewness of 1:2 is considered suitable. The relatively high errors that Nemoh outputs makes it hard to live up to requirements. Also the odd convergence when modelling with a skewness of 2:1 and 1:1 with Nemoh isn't preferable. For further analysis in this report Wamit will be used.

3.4 Boat Landing model

Modelling this model can be done in two different ways, using only one or two mesh files. The difference is when using one mesh file, the monopile and secondary structure is

together and the calculations consider them as a single 6-DOF construction from which reactions can be extracted. Using two mesh files, the mesh of the monopile and secondary structure are separate and is considered as two 6-DOF constructions for a total of 12 DOF. In this project both methods are utilised and they are compared in order to validate that resulting reactions equals each other.

3.4.1 Meshing

In the previous section, the mesh for the monopile was selected and in this model the secondary structure also needs to be meshed. Because the secondary structure is significantly smaller than the monopile, it would results in an excessive amount of elements if this would be meshed using the same conditions as for the monopile. Because the forces from the secondary structure also would contribute with relatively small amount of the total forces, a mesh with a larger skewness and lesser discretion of the semi-circle would be allowed. A mesh for the secondary structure with a discretion of the semi-circle of 8 and a skewness of 4 would give a mesh with 464 elements for the secondary structure, which seems reasonable considering the mesh of the monopile consist of 360 elements. Illustrations of the chosen mesh are shown in Fig 3.11

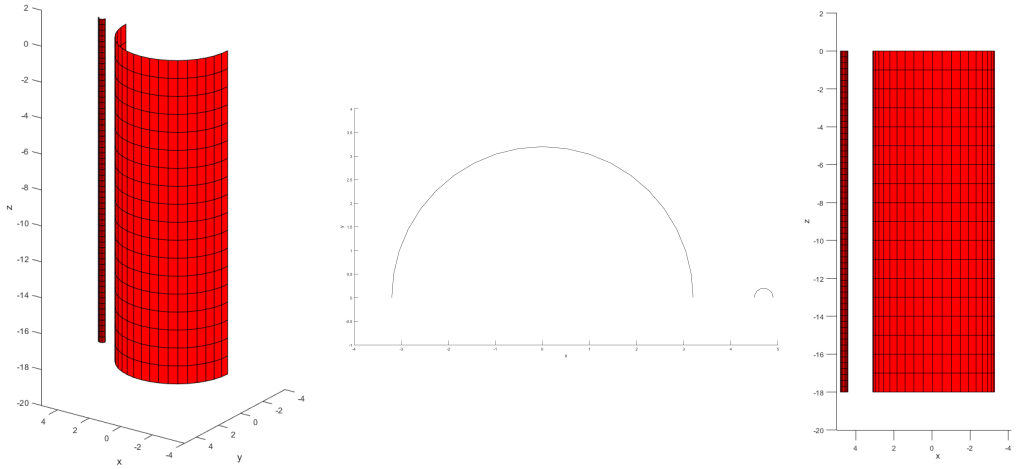

Fig 3.11. Views of Mesh for Boat Landing model. Perspective - Top view - Front view.

3.4.2 One or two mesh files

In this section, results from the calculations with one and two mesh files will be compared. Because the structures are not hit by the wave at the same time there is a phase shift between the two forces in the x-direction for the separated mesh and this needs to be considered. The wave force as stated in Eq. (2.2) can also be expressed as complex numbers shown in Eq. (3.1), which is the method that Wamit used to represent its results. The complex notation doesn't have the phase and therefore can the results simply be added together with basis of the super position principle.

$$F(t) = Re\left(a_f e^{i\omega t}\right) = |a_f|\cos(\omega t + \delta) \tag{3.1}$$

$F(t)$	Force	[N]
a_f	Force amplitude	[N]

It can be seen on Fig 3.12 that there is no significant between using one or two mesh files. Therefore it would be safe to use results from either model depended on the purpose of compare.

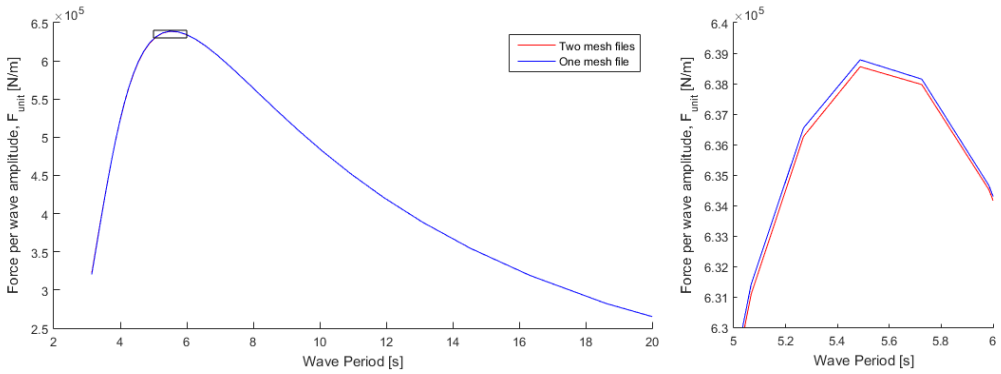

Fig 3.12. Comparison between one and two mesh files.

3.4.3 Forces on secondary structure

It is also relevant to consider the magnitude of the forces on the secondary structure compared to the monopile in order to determine if BEM is a viable method to determine the forces on the secondary structure. On Fig 3.13 the forces on both the monopile and secondary structure is plotted. The forces on the secondary structure is barely visible, so on Fig 3.14 there is zoomed in on the force on the secondary structure.

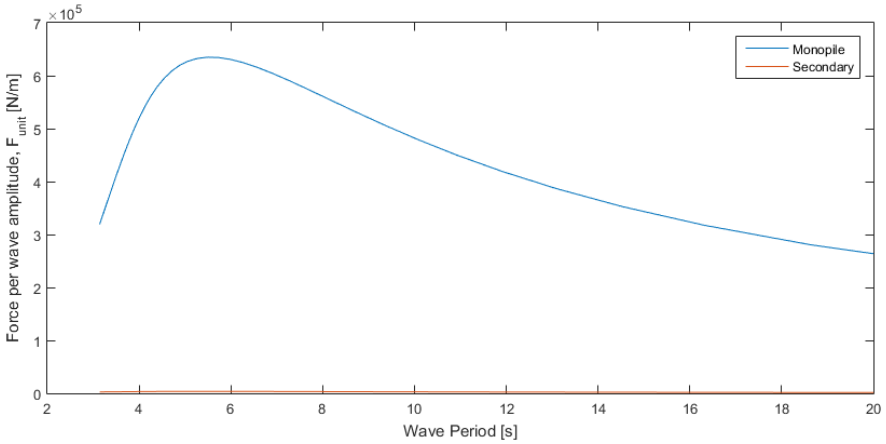

Fig 3.13. Forces on monopile and secondary structure.

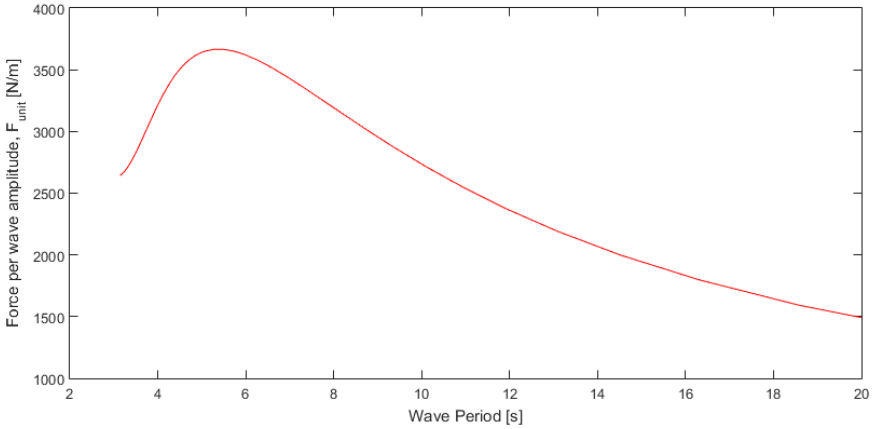

Fig 3.14. Zoom on the forces on the secondary structure.

The forces on the secondary structure are more than 100 times smaller than the forces on the monopile and could under normal circumstances be neglected. By only considering the secondary structure, it would drag dominated and BEM don't consider drag and forces on the secondary structure in real life would probably be larger because of drag. Therefore the force obtained from the model with two mesh files will be compared with results from the CFD-method and the physical model tests, which both consider drag.

3.4.4 Influence of secondary structure

It is also relevant to investigate the influence of the secondary structure on the forces on the monopile. This can be done comparing the results from the Monopile model and Boat Landing model with two mesh files and only consider the forces on the monopile. In Fig 3.15 the forces are plotted. It can be seen that the difference is less than 0.5 % and this can almost be counteracted by model uncertainties.

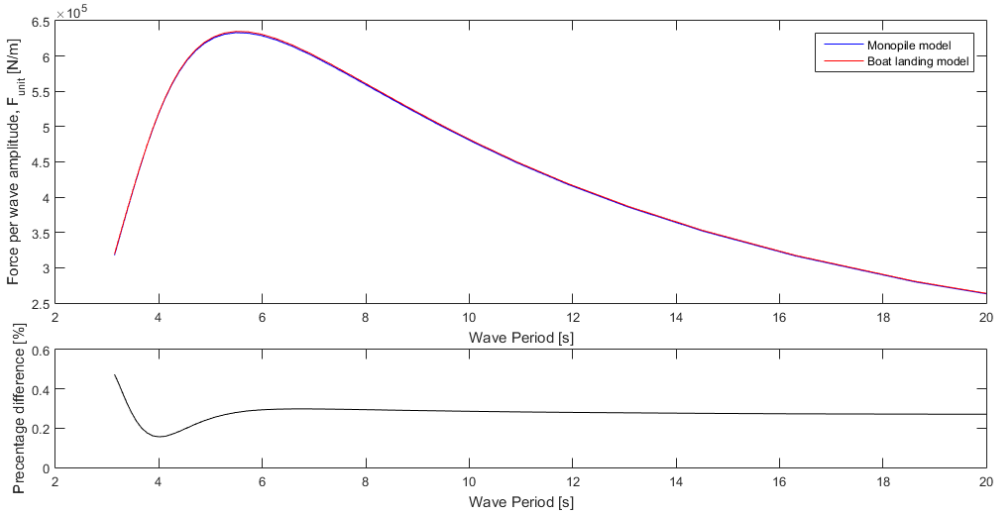

Fig 3.15. Force on monopile with and without secondary structure.

The increase of the total forces on the Boat Landing model can also be compared with the Monopile model to determine how much the secondary contribute to the total forces.

On Fig 3.16 this is plotted. The difference is here less than one percent, which can be considered insignificant.

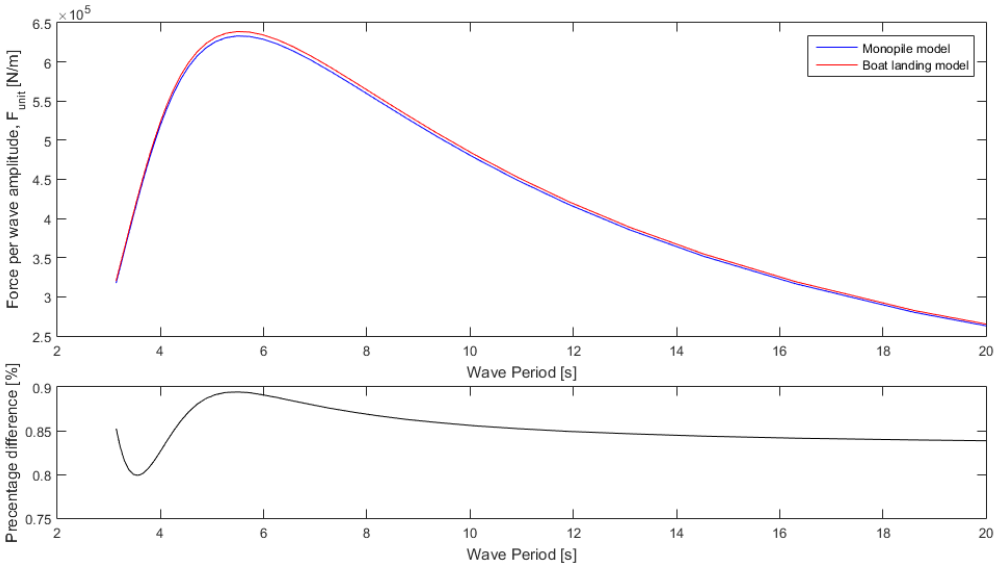

Fig 3.16. Total force on construction with and without secondary structure.

It is also relevant to consider the influence of the monopile on the forces on the secondary structure. On Fig 3.17 it can be seen that there is a significant difference. When the monopile is present the forces on the secondary structure is approx. 50 % larger compared to when there isn't any monopile.

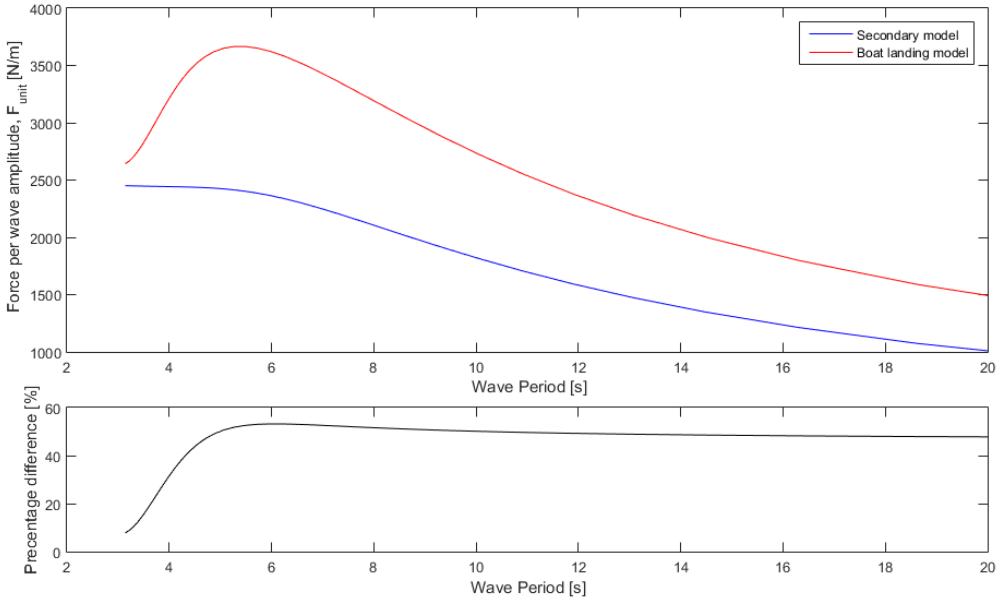

Fig 3.17. Force on secondary structure with and without monopile.

CFD-METHOD 4

In this chapter the construction is analysed using CFD simulations.

4.1 Theory

The problem that needs to be solved in this project is a free-surface problem and for this purpose the Volume of Fluid (VOF) method can be used for the analysis.

VOF is a method for tracking and locating the free surface and in an Eulerian approach. The advantage of this method is that it only adds one additional variable to located the free surface. This is done using a fraction function, F, which is a scalar function that specifies the amount of fluid in a cell with a value between zero and one. F can be in three states.

- $F = 0$, the cell is empty
- $F = 1$, the cell is completely full
- $0 < F < 1$, the cell is partially full

The free surface would in most cases intersect a mesh cell in the domain and this particular cell would therefore not be either full or empty. I can be deduced that the free surface has to be in a cell with $0 < F < 1$. On Fig 4.1 this is illustrated.

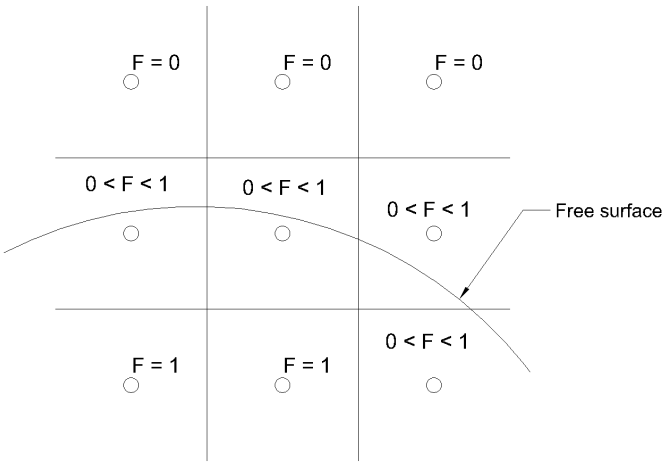

Fig 4.1. Locating free surface with fraction function.

The VOF is only for locating the free surface and the Navier-Stokes also have to be solved in order to describe the flow in the control volume.

4.1.1 Program

To make the CFD simulations, the program Star-CCM+ version 10.06 is used. One of the advantages of this program is that it is possible to generate waves using so-called VOF-waves. This can generate different types of waves and in order consider non-linear effects of the waves a 5th order stokes regular waves are used. This is the most non-linear regular wave the program can generate.

4.2 Model considerations

In order to make a good model many different aspects needs to be considered when making the model in order to produce acceptable results. According to CD-adapco [2015] there is a series of best practices which are used for this project. The model is made using measures based on the physical model test. This is done in order to avoid possible scaling errors between model tests and CFD simulations.

4.2.1 Domain size

When modelling the domain it is important to consider the flow within the domain and in this case the waves. The waves used are based on the waves measured in the model tests, listed in Table 5.1.

The domain is modelled such that there would be approx. one wave length before the construction, one wave length after before wave damping starts and one wave length of damping. This totals to three wave lengths in the x-direction. In y-direction the domain is sized of what is assumed appropriate. For z-direction the water level and wave height are the main things to consider. From the bottom to MWL is 0.45 m as stated by the model and from MWL to top the domain is chosen to make sure waves would stay in the domain and possible splash from hitting the construction wouldn't leave the domain.

Because there are three different wave periods of the waves and this is a key parameter for the wave length, three different domain were made with different length. These are listed with dimensions are listed in Table 4.1.

Model	**Wave length** [m]	**x-direction** [m]	**y-direction** [m]	**z-direction** [m]
Waves 1-2-3	2.15	6.00	0.64	0.75
Waves 4-5-6	3.66	10.48	0.64	0.75
Waves 7-8-9	5.07	14.96	0.64	0.75

Table 4.1. Domain sizes for the different CFD-models.

4.2.2 Mesh

One of the most important consideration must be the mesh. If the mesh is too coarse, the waves will not be modelled sufficiently well and the results would not be usable. If the mesh is too fine the computational time would be very long. In order to model the waves sufficiently well the mesh around the waves should sized according to the wave. The recommendations according to CD-adapco [2015] can be seen below.

	Element size
x-direction	1/80 of the wave length
y-direction	1/80 of the wave length
z-direction	1/20 of the wave amplitude

This modification of the mesh can be applied using volume control, which means that within a certain volume these are the mesh requirements. Therefore it is not necessary to model the entire domain with these conditions.

Star-CCM+ uses a method of meshing where the elements are halved in size and the requirement listed in the volume control is the maximum size, meaning the program would rather make a step finer than coarser. Therefore it is a good idea to choose the base size of the elements based on the sizes stated in the volume control for the wave, which is the important part. On Fig 4.2 - 4.4 illustrations of the mesh is shown.

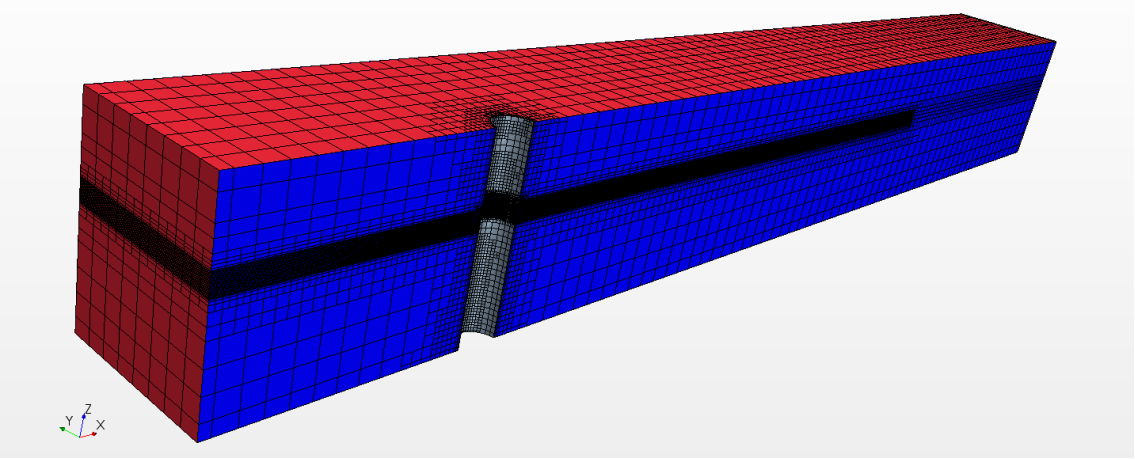

Fig 4.2. Illustration of the surface mesh of the domain and monopile model for Waves 1-2-3.

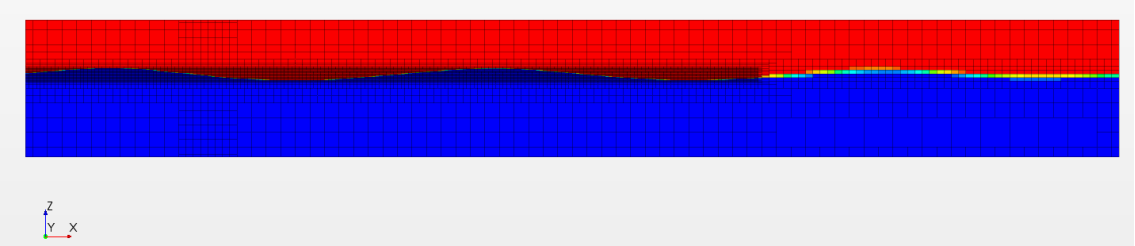

Fig 4.3. Illustration of the mesh in the domain with displayed volume fraction (Blue: F = 1 - Red: F = 0).

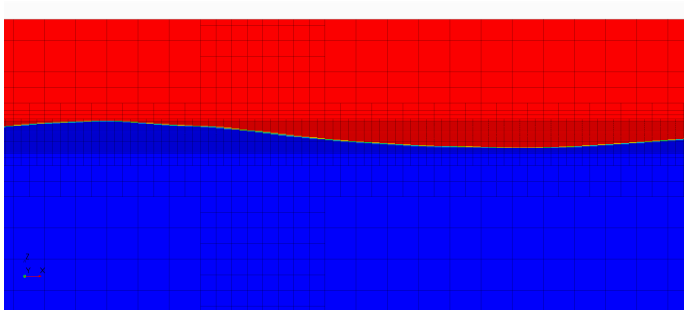

Fig 4.4. Illustration of the mesh near a wave with displayed volume fraction.

4.2.3 Wave Damping

The domain modelled is to be considered as a small section of a much larger domain and no wave reflection would occur, but this can happen in the model. Therefore it is good idea to have wave damping at outlet. This would extract energy out of the system that would in other cases be reflected. This can be done using a combination of implementing a damping term and making the mesh coarser at the outlet. The mesh damping can be seen on Fig 4.3.

4.2.4 Time-step

Having a appropriate time-step would make sure that the solver is stable and also that the wave are modelled correctly. If the time-step isn't set correctly, it could result in the modelled not converging and the residuals constantly increasing until the solver can't handle it. Following Eq. (4.1) stated by CD-adapco [2015] will give an appropriate time-step. Based on this a time-step $\Delta t = 0.005\,\mathrm{s}$ will be used for all models.

$$\Delta t = \frac{P}{2.4n} \tag{4.1}$$

Δt	Time-step	[s]
P	Wave Period	[s]
n	Graduation of wavelength to mesh size in x-direction, e.g. n=80	[-]

4.2.5 Turbulence model

There are four turbulence models incorporated into Star-CCM+ which are:

- Spalart-Allmaras
- K-Epsilon
- K-Omega
- Reynolds Stress Transport

The four models all have pro and cons but for this project, the K-Epsilon model has been preferred. The reason for this that both K-Epsilon and K-Omega utilizes wall functions which interpolates the flow towards walls in the domain. This makes it possible to have more coarse mesh close to constructions, but without major compromises in the results.

Between K-Epsilon and K-Omega, the latter require more computational power, but can produce slightly better results, but not enough to be chosen over K-Epsilon.

Spalart-Allmaras has been considered to simple and performs poorly in flows with separation. Reynolds Stress Transport is much more computational heavy and was opted out on this point.

4.2.6 Symmetry

CFD-simulations are very time consuming and a method to reduce this is by using symmetry in the model. For the models with only the monopile this would not represent any issues, but the models with the secondary structure, it can be an issue. Using symmetry would cause that there would be two secondary structure, as seen on Fig 4.10, and therefore must the effect of the secondary structure on monopile be investigated. This will done by making a simulation using symmetry and a simulation with the full domain and compare the difference between the forces on the monopile. On the following figures the differences between modelling without and with symmetry is shown. The number of elements when not using symmetry is 578 450 elements and when using symmetry it is 191 401 elements which is a significant difference.

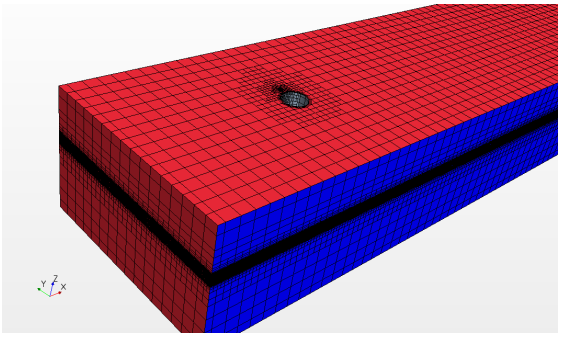

Fig 4.5. Mesh without symmetry.

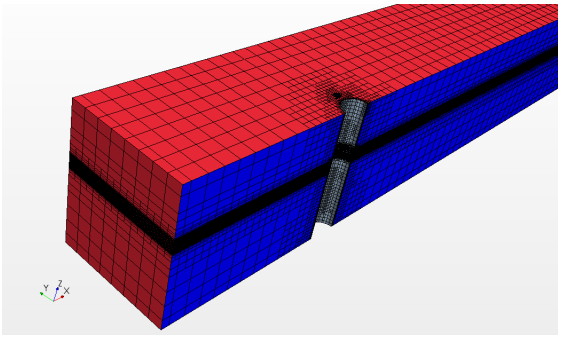

Fig 4.6. Mesh with symmetry.

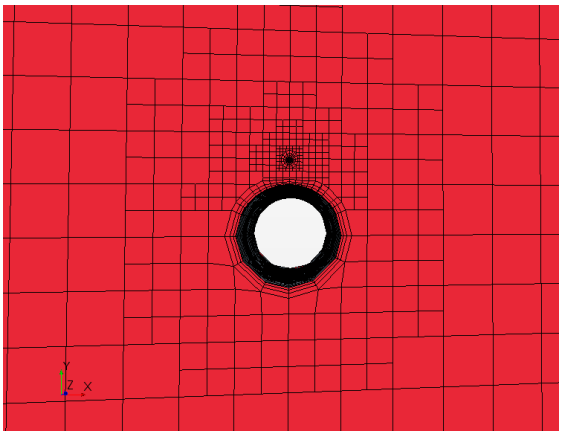

Fig 4.7. Mesh around model without symmetry.

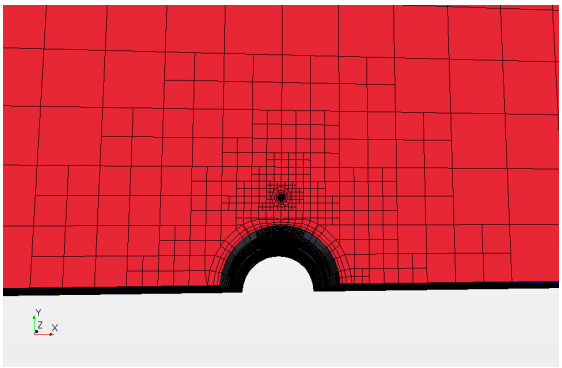

Fig 4.8. Mesh around model with symmetry.

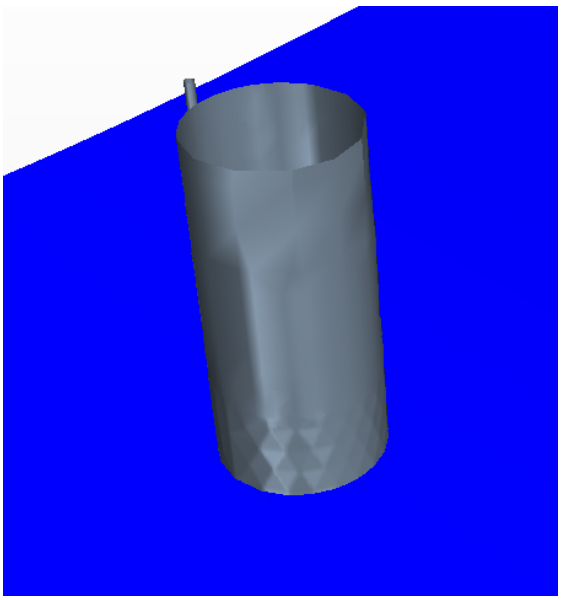

Fig 4.9. Model and free surface without symmetry.

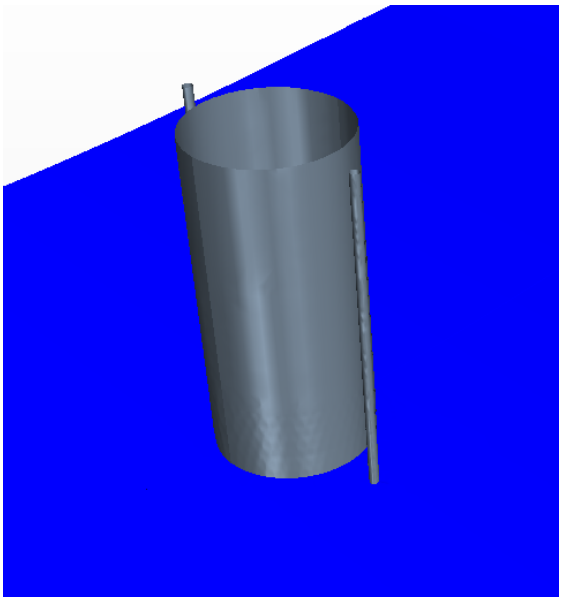

Fig 4.10. Model and free surface with symmetry.

4.3 Data treatment

In this section the data treatment of a simulation of Monopile model under excitation of Wave 2 is done as an example. Same procedure is done for all tests. The wave signal is determined from a simulation where the structure was not present in the domain. Wave signal and forces in x-direction can seen on Fig 4.11

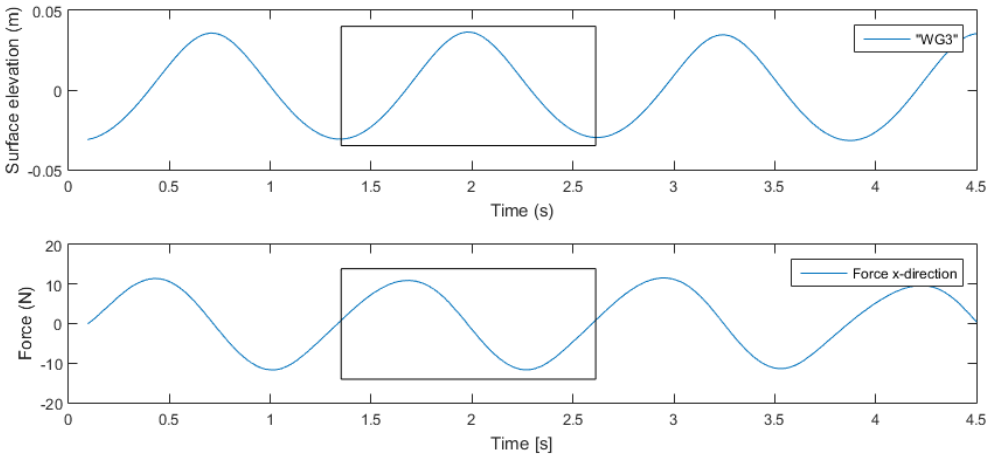

Fig 4.11. Wave signal and forces on the structure in x-direction.

The forces on the structure and the corresponding wave height is determined from a single wave. The chosen wave is indicated with a box that has the width of one wave period as seen on Fig 4.11. The values in this box are considered.

The wave height of the selected wave is determined by the distance between minimum and maximum amplitude of the wave signal. The maximum force, F_{max}, is maximum value of the force signal and for the selected wave it is indicated with a $\times$ on Fig 4.12.

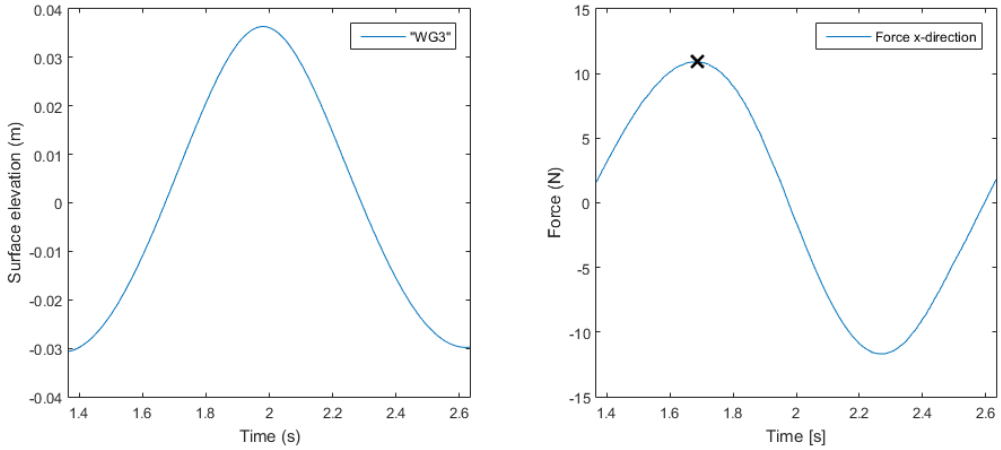

Fig 4.12. Zoom on the selected wave.

In order to being able to compare the results with the other methods, a force per wave amplitude is calculated using Eq. (4.2).

$$F_{unit} = \frac{F_{max}}{(H/2)} \tag{4.2}$$

F_{unit}	Force per wave amplitude	[N/m]
F_{max}	Maximum Force	[N]
H	Wave height	[m]

4.4 Results

4.4.1 Monopile model

The results from simulations of Monopile model are presented in Table 4.2 and plotted with MacCamy and Fuchs in Fig 4.13

Wave	**1**	**2**	**3**	**4**	**5**	**6**	**7**	**8**	**9**
H	0.032	0.067	0.243	0.026	0.065	0.248	0.027	0.053	0.207
F_{max}	5.210	10.909	40.363	3.338	8.531	42.733	2.833	5.902	32.008
F_{unit}	326.814	324.755	331.839	257.867	262.985	344.383	208.803	221.974	310.058

Table 4.2. Results from CFD simulation with monopile.

From Fig 4.13 it can be seen that the short and small waves which causes the forces to be inertia dominated, the forces from the CFD-simulations aligns close to the solution by MCF. When the waves become long and large and drag thereby have more influence, the forces increases above solution from MCF.

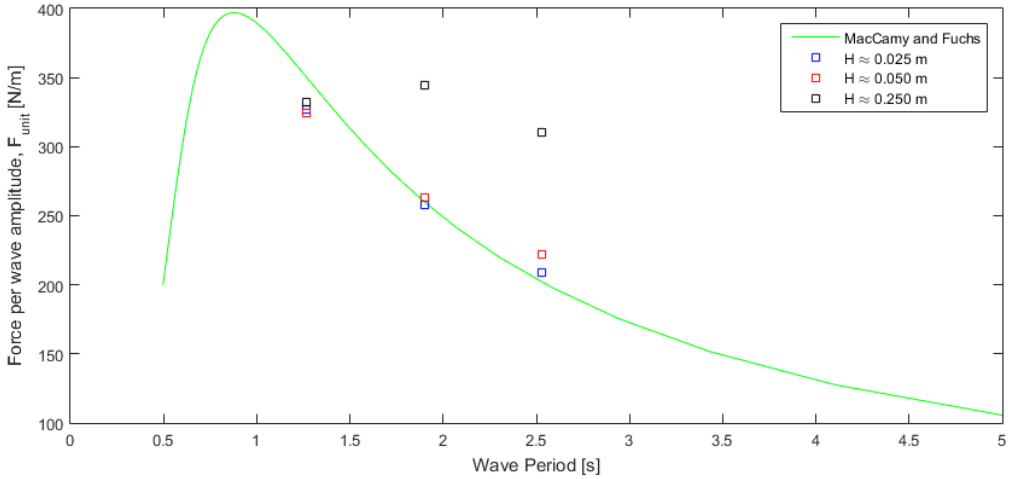

Fig 4.13. Results from CFD simulation with monopile plotted with MCF.

4.4.2 Boat Landing model

For this model the results are listed in Table 4.3. In this table, the difference between the forces on the monopile and the secondary structure are also shown and

	Wave	**1**	**2**	**3**	**4**	**5**	**6**
	H	0.032	0.067	0.243	0.026	0.065	0.248
Monopile	$F_{max,m}$	5.265	11.009	40.983	3.383	8.624	43.638
	$F_{unit,m}$	330.245	327.747	336.937	261.338	265.863	351.674
Secondary	$F_{max,s}$	0.035	0.110	1.363	0.026	0.121	2.005
	$F_{unit,s}$	2.171	3.261	11.206	2.025	3.724	16.156
	$F_{unit,m}/F_{unit,s}$	152.1	100.5	30.1	129.1	71.4	21.8
	Wave	**7**	**8**	**9**			
	H	0.028	0.053	0.207			
Monopile	$F_{max,m}$	2.868	5.908	32.584			
	$F_{unit,m}$	208.805	222.191	315.645			
Secondary	$F_{max,s}$	0.029	0.094	1.327			
	$F_{unit,s}$	2.089	3.517	12.850			
	$F_{unit,m}/F_{unit,s}$	100.0	63.2	24.6			

Table 4.3. Results from CFD simulation with monopile and secondary structure.

It is clear that larger and longer waves become more drag dominated and a larger share of the total forces can be contributed to the forces on the secondary structure. For Wave 1 the forces on the monopile is 150 times greater than on the secondary and for Wave 9 the forces on the monopile is only 25 times greater than on the secondary.

In relation to the consideration of symmetry in the model, tests show that there is difference of 5.3 % on the forces on the monopile and 3.7 % on the secondary structure. For both the results without symmetry are larger than with. This is relevant to notice when comparing and concluding on the results.

4.4.3 Influence of structure on waves

In this sections a number of figures illustrating the influence the structure has on the waves compared to undisturbed waves.

The first four figures shows results from a simulation with Wave 2, all for the same time-step. Fig 4.14 and 4.15 shows plots of the surface elevation as seen from above and Fig 4.16 and 4.17 show the volume fraction of water in a X-Z plane section through the middle of the construction. It can be seen that the construction has an influence on the waves, but the different isn't very big because Wave 2 is considered a small wave.

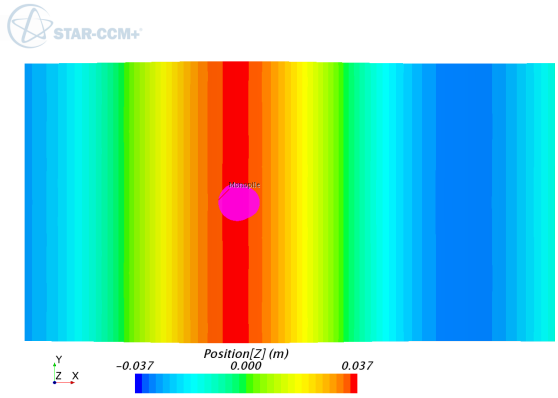

Fig 4.14. Plot of surface elevation without construction in domain.

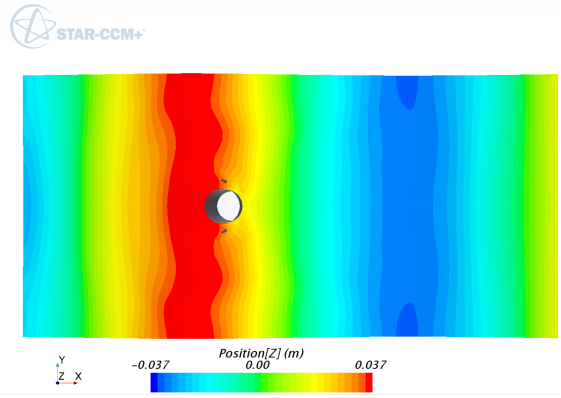

Fig 4.15. Plot of surface elevation with construction in domain.

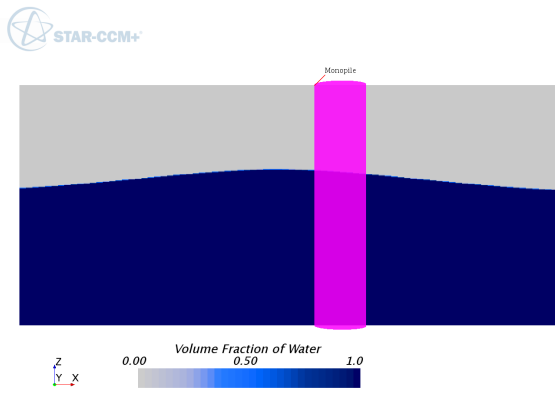

Fig 4.16. Plot of Volume Fraction of Water without construction in domain.

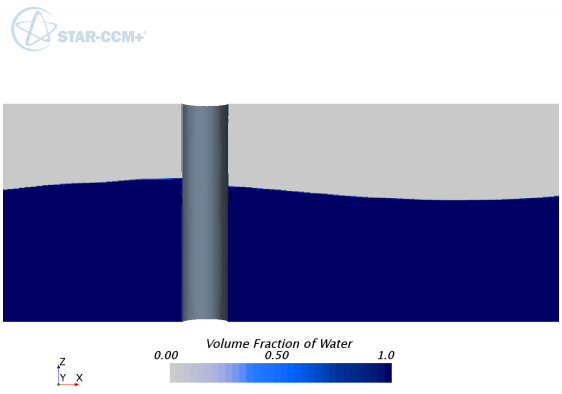

Fig 4.17. Plot of Volume Fraction of Water with construction in domain.

The next four figures show results from a simulation with Wave 3, all for the same time-step. Fig 4.18 and 4.19 shows plots of the surface elevation as seen from above and Fig 4.20 and 4.21 show the volume fraction of water in a X-Z plane section through the middle of the construction. Because Wave 3 is considered a large wave the differences are much clearer. It can be seen that a significant amount of run-up on the construction and in the wake of the construction the surface elevation is visibly lower. This would without a doubt have influence on the forces on the structure. I can also be seen on Fig 4.19 that to the side of the construction the surface elevation is larger than without the construction. This could be an effect of the reflected wave from the construction.

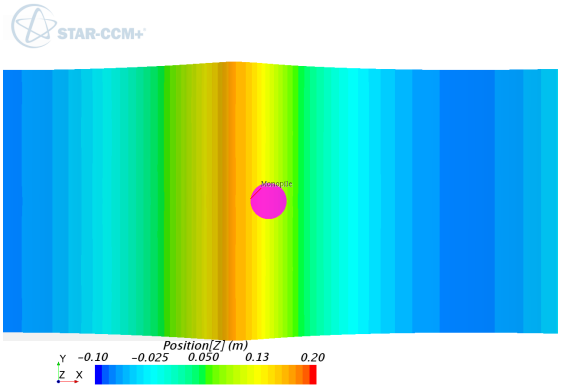

Fig 4.18. Plot of surface elevation without construction in domain.

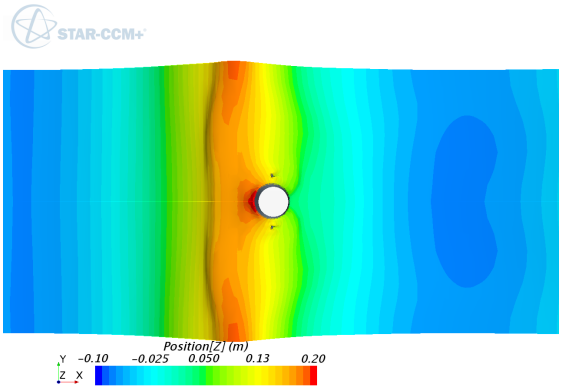

Fig 4.19. Plot of surface elevation with construction in domain.

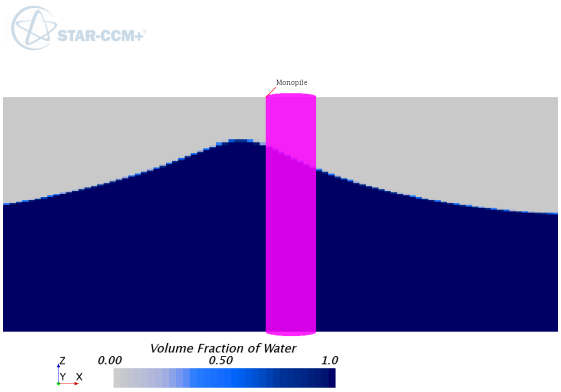

Fig 4.20. Plot of Volume Fraction of Water without construction in domain.

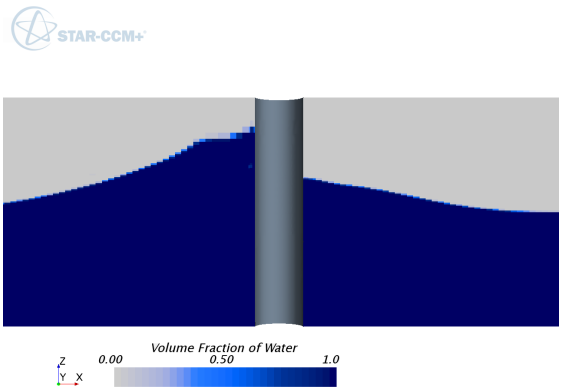

Fig 4.21. Plot of Volume Fraction of Water with construction in domain.

Comparison 5

In this chapter a comparison between the methods used will be made. Results from physical model test will be used in this comparison. These physical model tests were performed by a fellow student, Ammar Galib Al-Faili.

5.1 Physical model tests

In this section, a quick review of the model testing will be made. The model is scaled using Froude Number with a length factor of 40. The dimensions of the model are listed in Table 1.1. A picture of the model is shown on Fig 5.1. The test were performed in a wave basin located at Aalborg University and a layout of the basin can be seen on Fig 5.2. Worth mentioning is that during the test one of the paddles on the wave generator had a malfunction which wasn't discovered until afterwards and this might have had a influence on the results. This is will be considered in the conclusion.

Fig 5.1. Photo of the model used for testing.

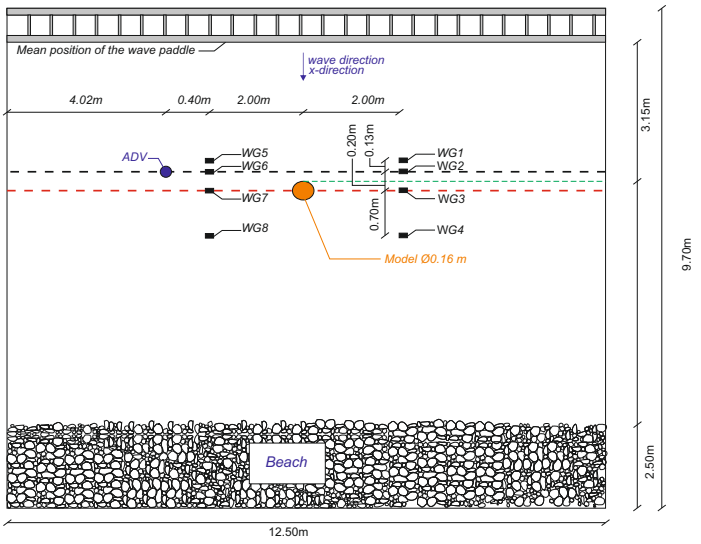

Fig 5.2. Layout of the wave basin for model testing.

Nine different wave condition with varying wave period and wave height were used in the physical model tests. The data treatment is done similar to the CFD model and can be seen in Appendix B.

18 test were performed with 9 on Monopile model and 9 on Boat Landing model. The waves used can be seen in Table 5.1. In order to keep the variables down, the waves measured from Monopile model and Boat Landing model are averaged and parameters calculated based on these data.

	Monopile		Boat Landing								
Test	H	T	H	T	H_{avg}	L	η_{max}	H/L	KC	Re	η_{max}/H
[-]	[m]	[s]	[-]	[m]	[s]	[m]	[m]	[m]	[-]	[-]	[-]
1	0.028	1.26	0.031	1.26	0.030	2.15	0.015	0.014	0.68	15609	0.50
2	0.060	1.26	0.067	1.26	0.065	2.15	0.034	0.030	1.47	33547	0.52
3	0.193	1.26	0.227	1.26	0.214	2.15	0.132	0.100	4.85	110789	0.62
4	0.028	1.90	0.024	1.90	0.026	3.66	0.014	0.007	0.80	12078	0.52
5	0.066	1.90	0.051	1.90	0.060	3.66	0.036	0.016	1.80	27296	0.61
6	0.244	1.90	0.216	1.90	0.235	3.66	0.165	0.064	7.13	107877	0.71
7	0.025	2.53	0.027	2.53	0.027	5.07	0.014	0.005	1.03	11702	0.53
8	0.056	2.53	0.062	2.53	0.060	5.07	0.034	0.012	2.33	26533	0.56
9	0.209	2.53	0.218	2.53	0.214	5.07	0.153	0.042	8.28	94101	0.72

Table 5.1. Waves used for Physical model test for Monopile model and Boat Landing model.

In order to be able to make visual comparison between the different waves, they have been placed in a matrix depend on wave height and wave period. Fig 5.3 shows the distribution of the tests. For each wave condition the corresponding Keulegan-Carpenter number, KC will be calculated. This is done using Eq. (5.1). KC shown in Table 5.1 is for the monopile. Other parameters such as the ratio H/L is calculated, which describes the steepness of the waves and η_{max}/H, which describes how non-linear the waves are. These parameters are shown in matrix form in Fig 5.4.

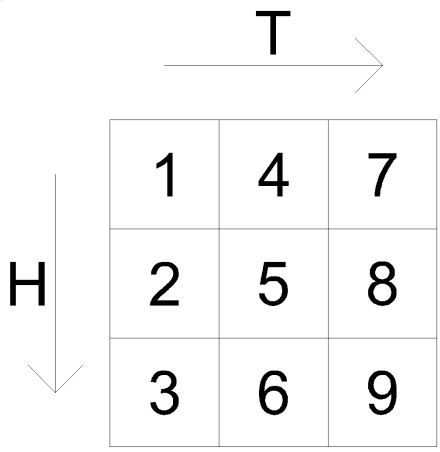

Fig 5.3. Distribution of the waves in matrix form.

$$KC = \frac{U_{max} T}{D} \tag{5.1}$$

U_{max}	Max horizontal velocity	[m/s]
T	Wave period	[s]
D	Diameter of construction	[m]

$KC \leq 5$	Potential theory usable
$KC > 5$	Potential theory not usable

The max horizontal velocity, U_{max} is based on linear 1. order theory.

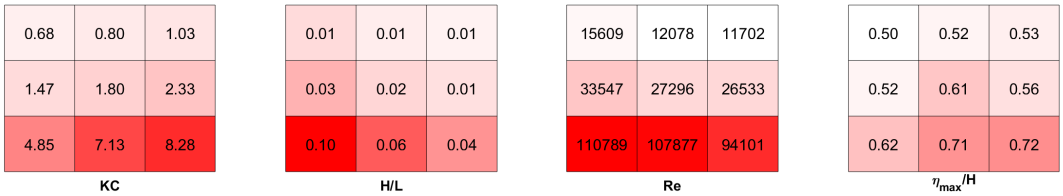

Fig 5.4. The parameters KC, H/L, Re, η_{max}/H from physical model tests in matrix form.

When increasing the wave height and wave period, this results in higher Keulegan-Carpenter number and more non-linear waves. This would cause MCF and BEM to no longer be valid because these are based on potential flow and linear theory. Therefore a deviation of the results from these would be expected when comparing with results from model test and CFD.

5.2 Monopile model

In order to have a comparison with BEM, F_{unit} from CFD and Model test are visualised as the relative to BEM. These can be seen in Fig 5.5.

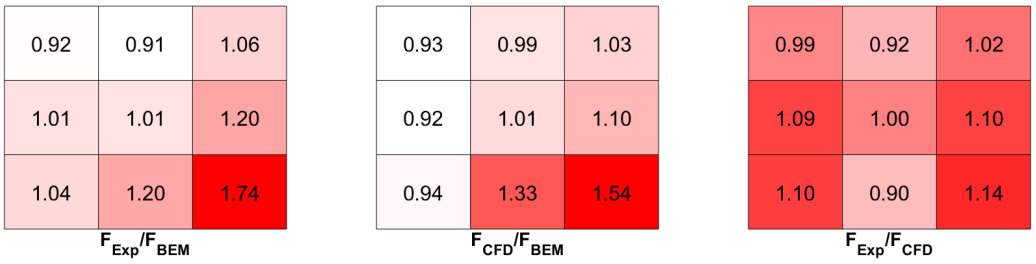

Fig 5.5. Forces from Model test, CFD and BEM relative to each other.

It can be seen on Fig 5.5 that the results from the model tests and CFD looks very similar. Also both looks to be depending on KC which was also expected.

Looking at the relative difference between the experimental results and CFD it can be seen that for this model there is only a little difference.

5.3 Boat Landing model

The forces considered are the combined forces from the monopile and secondary structure. Similar to Monopile model, it is expected that the forces from CFD and model tests would be higher when treating drag dominated waves. There is expected to be a slight increase in the forces, also for the waves where the monopile is inertia dominated, because the secondary structure would be drag dominated in all cases.

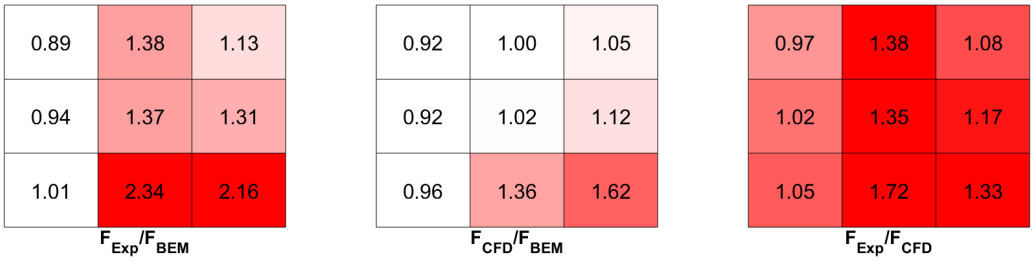

Fig 5.6. Forces from Model test, CFD and BEM relative to each other.

It can seen on Fig 5.6 that there is a similar difference between BEM and the other methods. Especially when the waves are drag dominated. It can also be seen that the results in the second column for the experiments looks to be much larger than expected. This could be due to an error with measurement of the test. The other results seems to follow the expectations. From the comparison between experiments and CFD shows that there are indications that CFD differs more from experiments with increasing KC.

It is also relevant to consider the force only on the secondary structure. Here there is only results from BEM and CFD available. Only looking on the secondary structure, it is also relevant to consider the Keulegan-Carpenter number for the secondary structure.

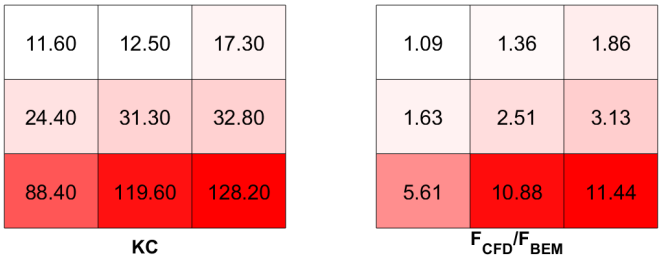

Fig 5.7. KC and Forces on secondary structure from CFD and BEM relative to each other.

KC for the secondary structure shows that it's drag dominated for all waves and particularly for the long and large waves. This drag dominance also clearly shows when comparing the forces between BEM and CFD, where Waves 8 and 9 gives 10 times larger forces than BEM calculates and this is a significant difference.

Conclusion 6

The main purpose of this project was to determine whether it is possible to use numerical models to determine the hydrodynamic forces on a monopile with secondary structures. Based on the models made it can be concluded that if it is the forces on the secondary structures that needs to be determined, then BEM isn't a usable method because the secondary structure would be drag dominated and this is beyond the validity of BEM. Even when considering the entire construction BEM still isn't a good method to use because for large waves the contribution from drag becomes so significant that BEM only estimates forces with a magnitude half of that produced from physical model tests.

Looking at the CFD models, they produce results which get closer to the results from the physical model test. But still there are some indication that the CFD models are sensitive to conditions with high Keulegan-Carpenter number. This could be a result of the chosen turbulence model and another turbulence model might be able to deal with higher Keulegan-Carpenter number. But CFD is a more accurate method of determining the forces on a monopile with secondary structure than BEM, but it is also much more time consuming.

This project shows that there are possibilities in using CFD models in order to determine forces on off-shore construction, but not everything have been investigated in this project and further studies needs to be done in order definitively determine the viability of these methods.

Further Studies

In this section a couple of the things that could be investigate further are mentioned in order to show what the next step could be.

As mentioned in Section 4.2 only one turbulence model was used in the CFD models for this project. An investigation into the influence of turbulence model could a valuable because if another turbulence model would model the flow better than the one used, then this might lead to more accurate determination of the forces in the model.

Another thing worth investigating is the placement of the secondary structure relative to the monopile. In this project only one placement was analysed, but it might be that another placement could be more critical for both the total forces, forces on the monopile, and forces on the secondary structure. Placements relative to the monopile could be in front, behind, or placed so the wave hit the secondary and monopile at the same time. The distance to the monopile could also be changed to see if placing the secondary structure closer or further from the monopile could lead to a decrease in the forces.

It could also be beneficial to analyse the influence of the surface roughness of the monopile and secondary structure. Knowing that for some wave conditions the

construction would be drag dominated, would lead to the surface roughness having a significant influence on the forces. This surface roughness would correspond to marine growth on the construction and therefore something that should be expected during its lifetime.

Knowing that there might have been a critical error during the physical model test caused be the malfunctioning wave generator, it might be a good idea to make new model tests to have for comparison in future analysis.

This project only utilised MacCamy and Fuchs as the analytical solution, but knowing that for part of the conditions drag had an influence, then it could be advantageous to make comparison to Morison equation which consider both drag and inertia forces.

Bibliography

Andersen et al., 2014. Thomas Lykke Andersen, Peter Frigaard and Hans F. Burcharth. *Lecture notes for the course in Water Wave Mechanics.* ISSN 1901-7286. Aalborg University - Department of Civil Engineering - Water and Soil, 2014. Chapter 3: Linear Wave Theory.

CD-adapco, 2015. CD-adapco. *User Guide - STAR-CCM+® 10.06.* CD-adapco, 2015.

COWI, 2015. COWI. *Full circle solutions for Wind Farms.* 021-1700-034e-12a. Kailow Graphic, 2015.

COWI, 2010. COWI. *London Array.* Youtube Video, 2010.

DNV-RP-C205, 2010. DNV-RP-C205. *DNV-RP-C205: Environmental Conditions and Environmental Loads.* DNV-RP-C205. Det Norske Veritas, 2010.

IEC 61400-3, 2009. IEC 61400-3. *Wind turbines - Part 3: Design requirements for offshore wind turbines.* IEC 61400-3:2009. Dansk Standard, 2009.

LHEEA, 2016. Énergétique et Environnement Atmosphérique LHEEA, Laboratoire de recherche en Hydrodynamique. *Nemoh.* URL: `http://lheea.ec-nantes.fr/doku.php/emo/nemoh/start`, 2016. Downloaded: 23-02-2016.

MacCamy and Fuchs, 1954. R.C. MacCamy and R.A. Fuchs. *Wave forces on piles : A diffraction theory.* Department of The Army, Corps of Engineers, 1954.

Sarpkaya and Isaacson, 1981. Turgut Sarpkaya and Michael Isaacson. *Mechanics of wave forces on offshore structures.* Van Nostrand Reinhold Co., New York, 1981. Chapter 6: Wave Forces on Large Bodies.

Results Convergence Monopile Ratio 1:1

A

Mesh Name	No. of elements	Error Nemoh [%]	Error Wamit [%]
Mesh−3	18	4.83	7.85
Mesh−4	32	0.96	4.49
Mesh−5	45	0.86	3.06
Mesh−6	66	1.19	2.11
Mesh−7	91	1.35	1.55
Mesh−8	120	1.41	1.19
Mesh−10	180	1.38	0.78
Mesh−12	264	1.28	0.54
Mesh−14	364	1.17	0.40
Mesh−16	464	1.05	0.31
Mesh−20	720	0.86	0.20

Table A.1. Meshes with the error from both Nemoh and Wamit compared to MCF.

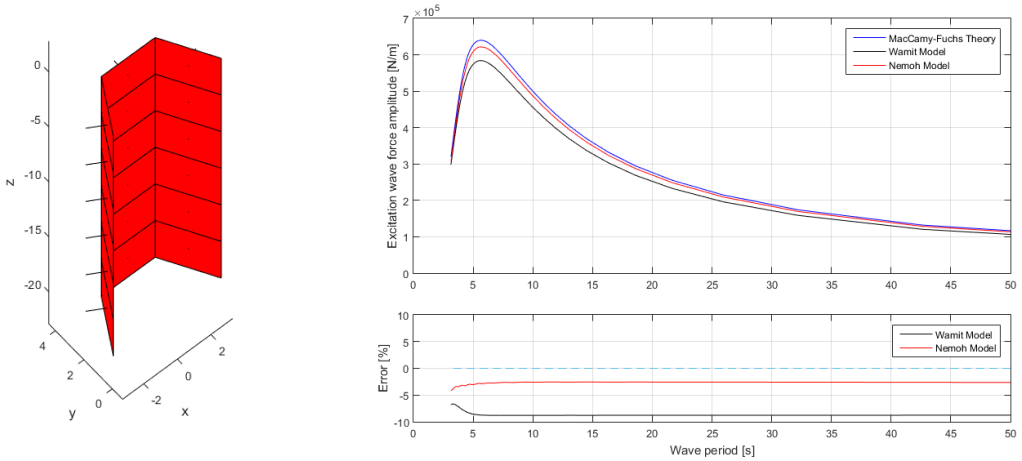

Fig A.1. Mesh 3 and the force from Nemoh and Wamit compared to McCamy-Fuch.

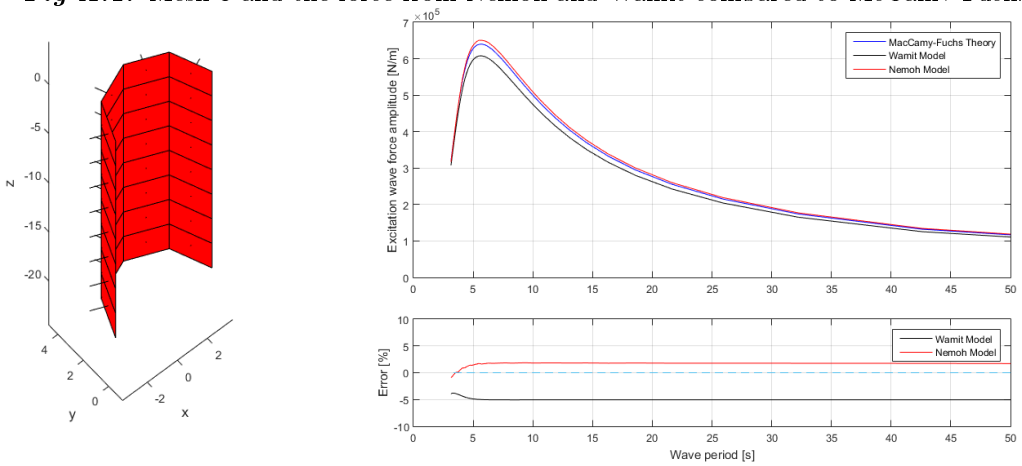

Fig A.2. Mesh 4 and the force from Nemoh and Wamit compared to McCamy-Fuch.

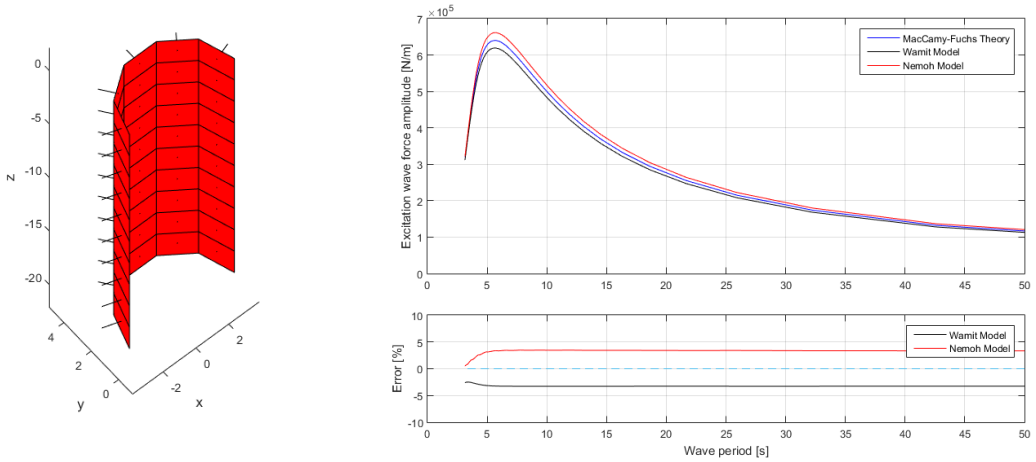

Fig A.3. Mesh 5 and the force from Nemoh and Wamit compared to McCamy-Fuch.

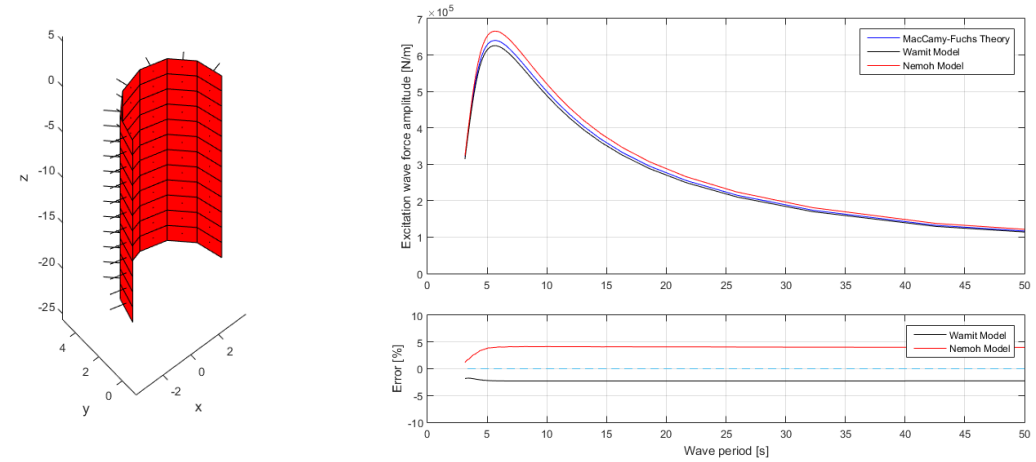

Fig A.4. Mesh 6 and the force from Nemoh and Wamit compared to McCamy-Fuch.

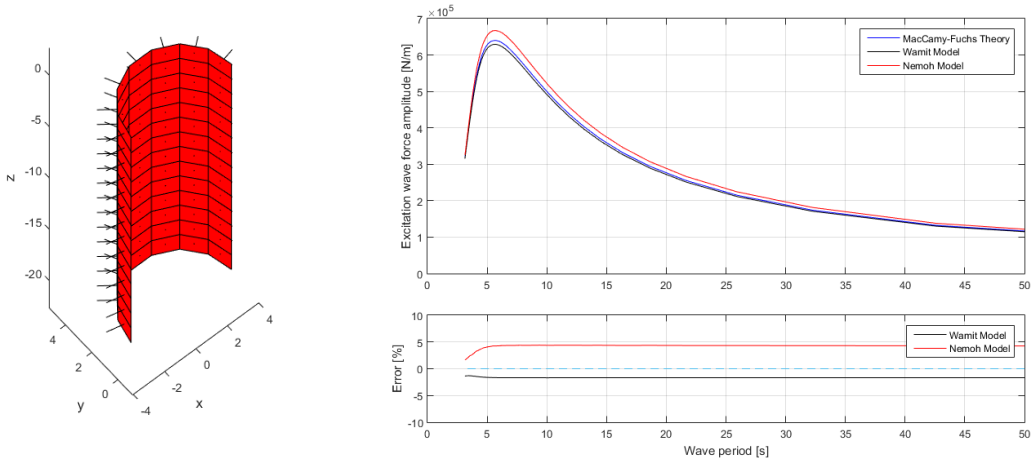

Fig A.5. Mesh 7 and the force from Nemoh and Wamit compared to McCamy-Fuch.

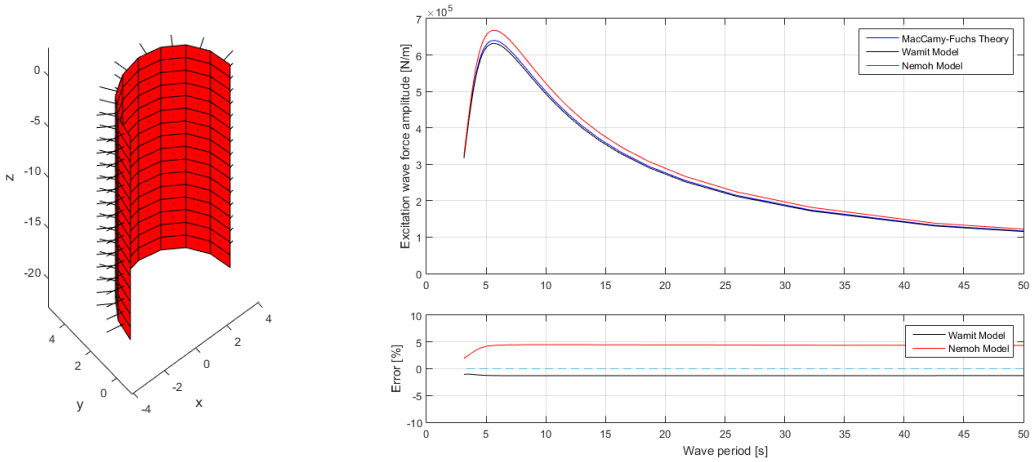

Fig A.6. Mesh 8 and the force from Nemoh and Wamit compared to McCamy-Fuch.

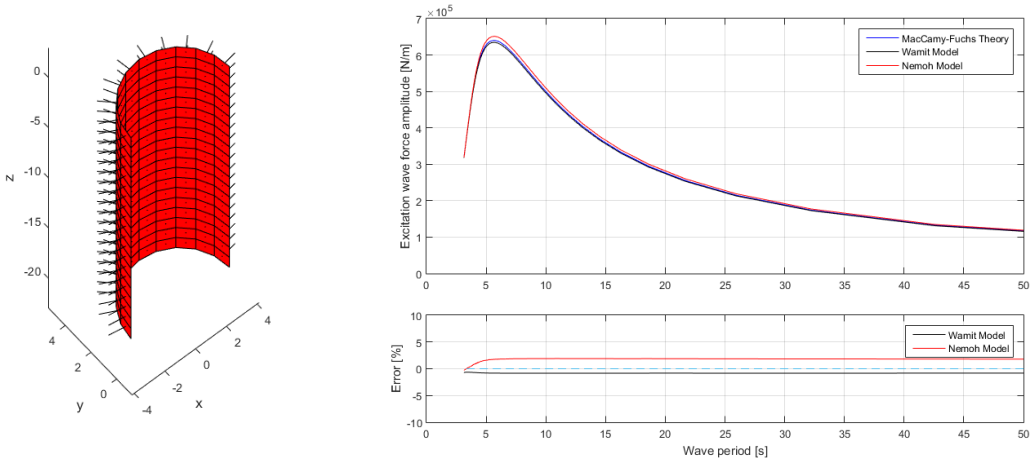

Fig A.7. Mesh 10 and the force from Nemoh and Wamit compared to McCamy-Fuch.

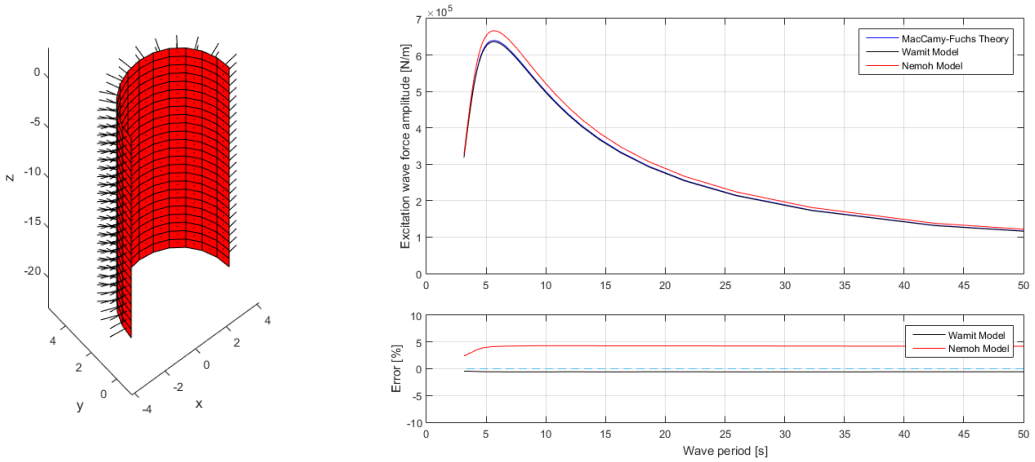

Fig A.8. Mesh 12 and the force from Nemoh and Wamit compared to McCamy-Fuch.

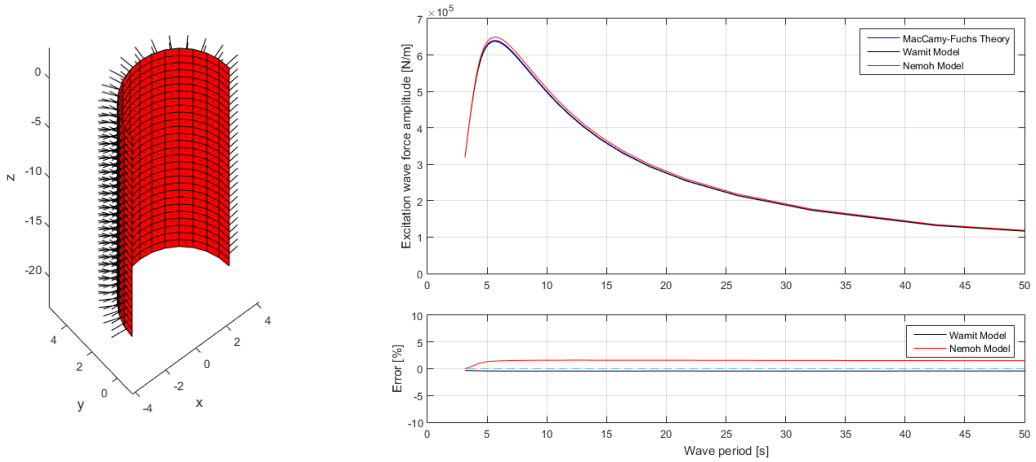

Fig A.9. Mesh 14 and the force from Nemoh and Wamit compared to McCamy-Fuch.

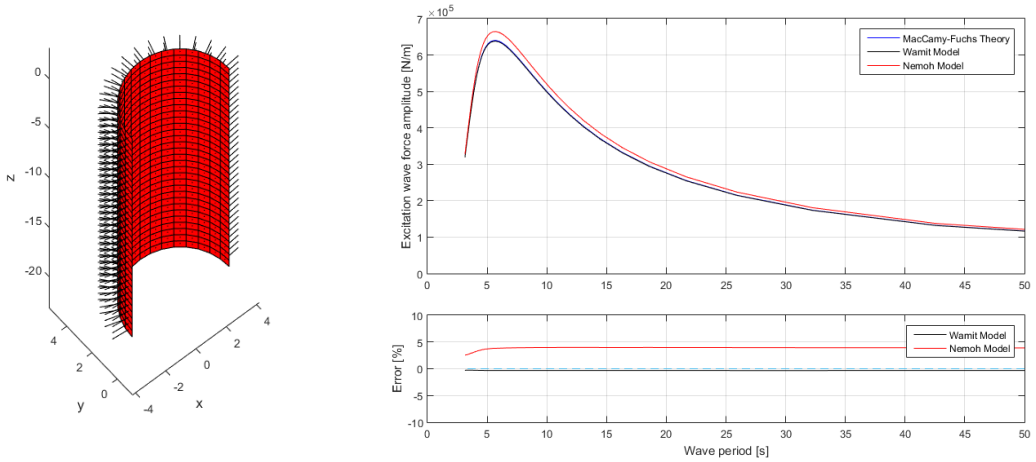

Fig A.10. Mesh 16 and the force from Nemoh and Wamit compared to McCamy-Fuch.

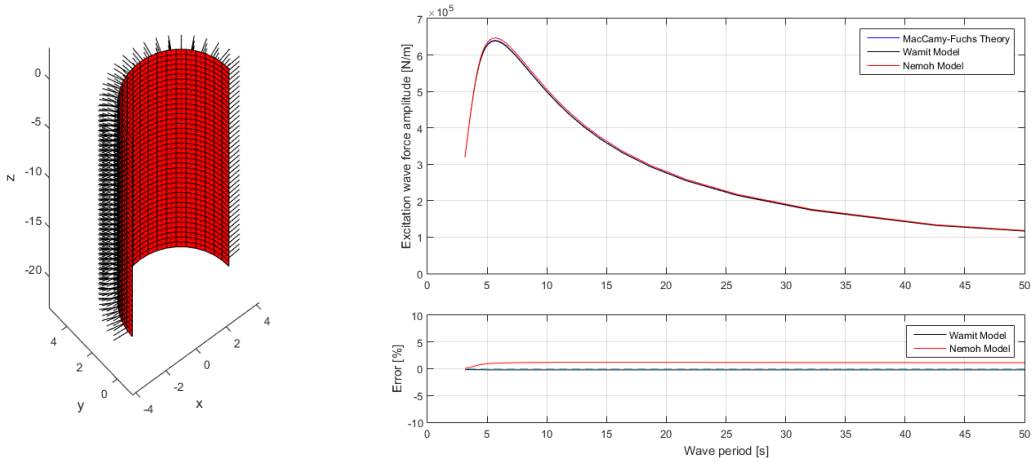

Fig A.11. Mesh 20 and the force from Nemoh and Wamit compared to McCamy-Fuch.

Data treatment of Experiments, Monopile Model

B

The data and script used for this data treatment can be found in Annex IV. The script is MichaelLoad.m

In this script a t_{chosen} is used for each wave. These are listed below:

Wave 1	Wave 2	Wave 3	Wave 4	Wave 5	Wave 6	Wave 7	Wave 8	Wave 9
11.7	11.7	11.7	13.7	16.7	12.7	11.7	11.7	11.7

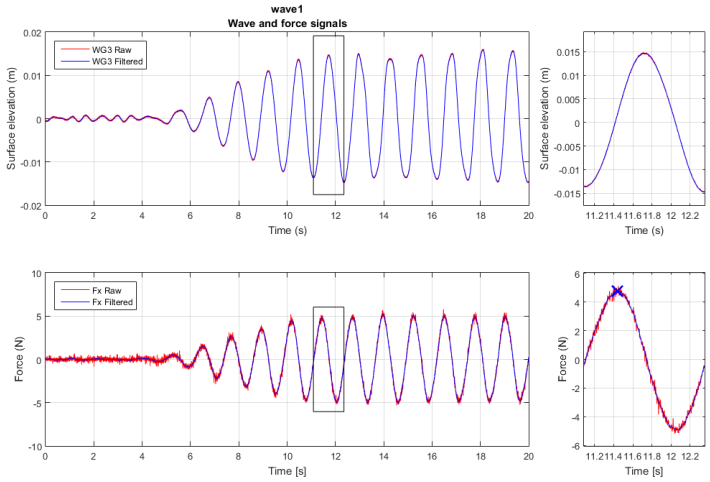

Fig B.1. Time series of surface elevation and force for Wave 1. With selected wave.

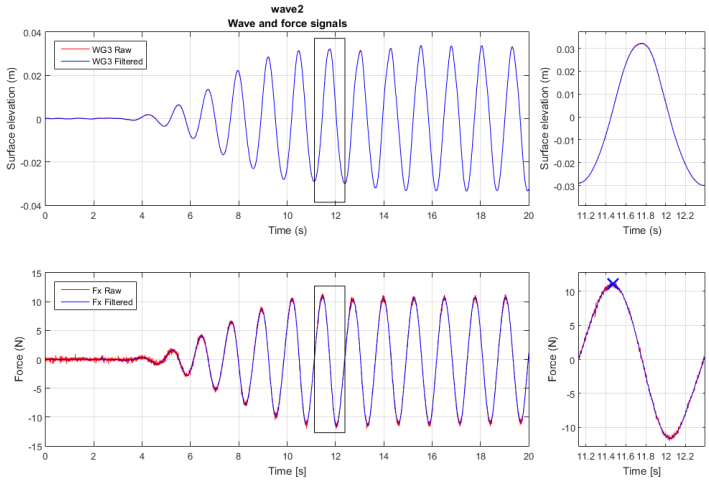

Fig B.2. Time series of surface elevation and force for Wave 2. With selected wave.

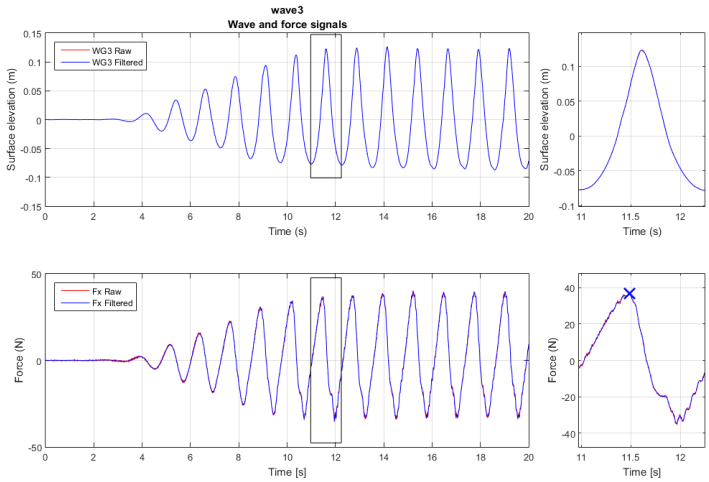

Fig B.3. Time series of surface elevation and force for Wave 3. With selected wave.

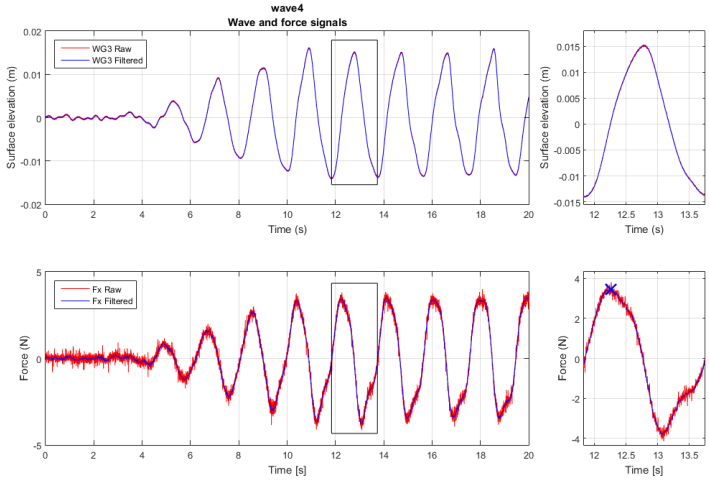

Fig B.4. Time series of surface elevation and force for Wave 4. With selected wave.

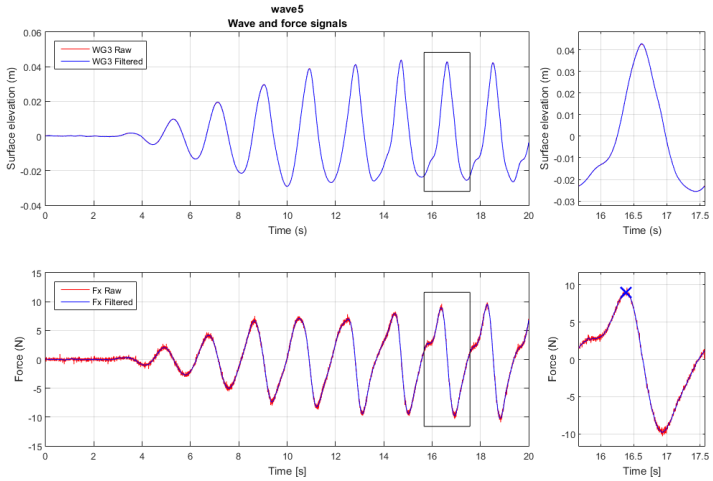

Fig B.5. Time series of surface elevation and force for Wave 5. With selected wave.

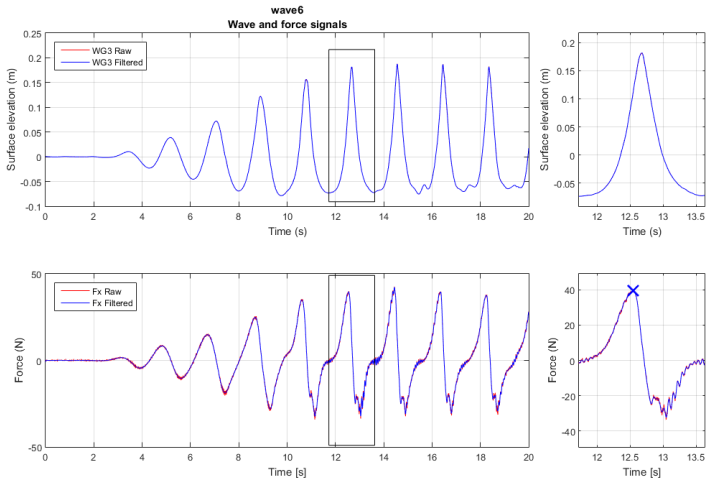

Fig B.6. Time series of surface elevation and force for Wave 6. With selected wave.

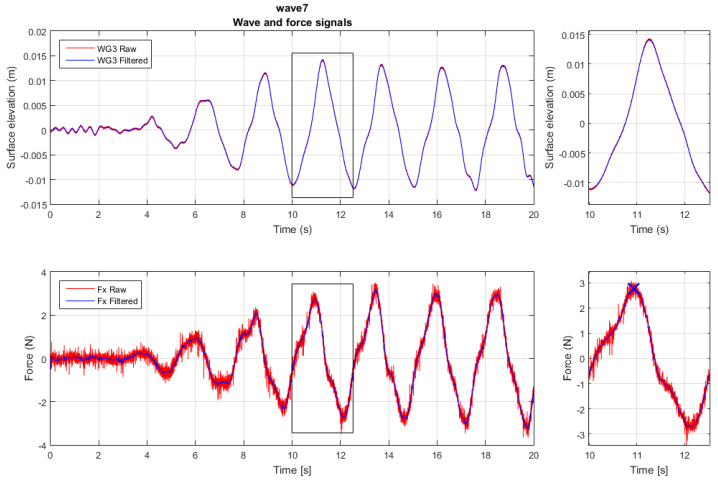

Fig B.7. Time series of surface elevation and force for Wave 7. With selected wave.

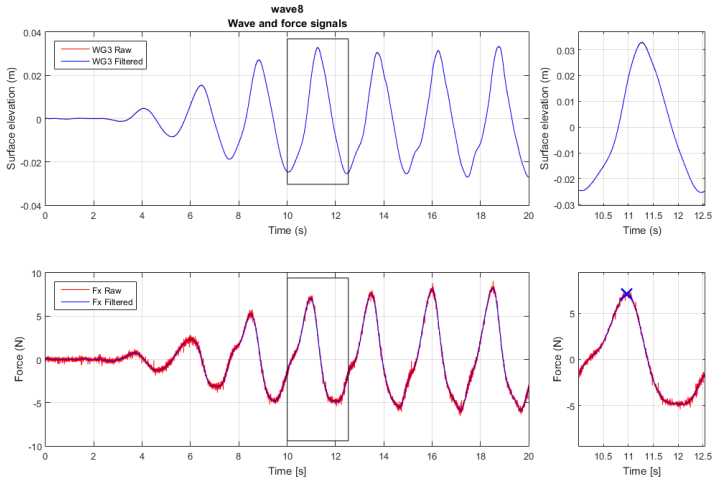

Fig B.8. Time series of surface elevation and force for Wave 8. With selected wave.

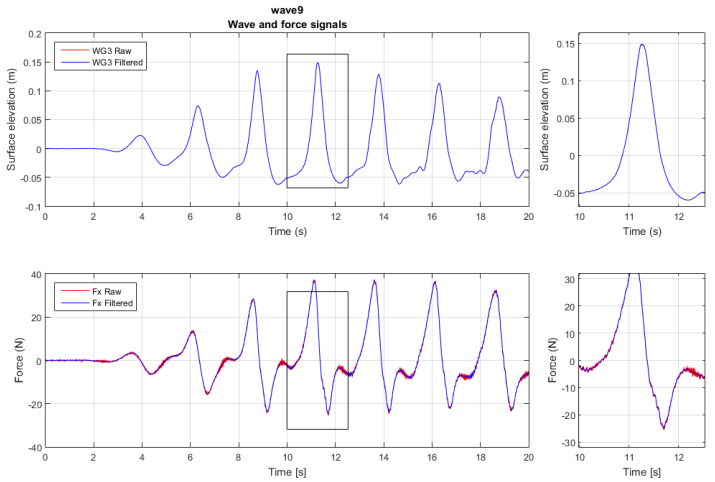

Fig B.9. Time series of surface elevation and force for Wave 9. With selected wave.

Annex Disc C

I **MacCamy-Fuchs** - *MATLAB scripts for calculating MacCamy-Fuchs*

II **Buoundary Element Method** - *Models for BEM calculations*

III **CFD** - *Models and Data from CFD-simulations*

IV **Physical Model Tests** - *Data from Physical Model Tests and scripts for analysis*

V **Comparison** - *Scripts for plotting figures for Comparison*